Neurobiology of Disease

$\alpha_2\delta$-1 Gene Deletion Affects Somatosensory Neuron Function and Delays Mechanical Hypersensitivity in Response to Peripheral Nerve Damage

Ryan Patel,[1]* Claudia S. Bauer,[1]* Manuela Nieto-Rostro,[1]* Wojciech Margas,[1] Laurent Ferron,[1] Kanchan Chaggar,[1] Kasumi Crews,[1] Juan D. Ramirez,[2] David L. H. Bennett,[2] Arnold Schwartz,[3] Anthony H. Dickenson,[1] and Annette C. Dolphin[1]

[1]Department of Neuroscience, Physiology and Pharmacology, University College London, London, WC1E 6BT, United Kingdom, [2]Nuffield Department of Clinical Neurosciences, John Radcliffe Hospital, University of Oxford, Oxford, OX1 2JD, United Kingdom, and [3]University of Cincinnati, College of Medicine, Cincinnati, Ohio 45229

The $\alpha_2\delta$-1 subunit of voltage-gated calcium channels is upregulated after sensory nerve injury and is also the therapeutic target of gabapentinoid drugs. It is therefore likely to play a key role in the development of neuropathic pain. In this study, we have examined mice in which $\alpha_2\delta$-1 gene expression is disrupted, to determine whether $\alpha_2\delta$-1 is involved in various modalities of nociception, and for the development of behavioral hypersensitivity after partial sciatic nerve ligation (PSNL). We find that naive $\alpha_2\delta$-1$^{-/-}$ mice show a marked behavioral deficit in mechanical and cold sensitivity, but no change in thermal nociception threshold. The lower mechanical sensitivity is mirrored by a reduced *in vivo* electrophysiological response of dorsal horn wide dynamic range neurons. The $Ca_V2.2$ level is reduced in brain and spinal cord synaptosomes from $\alpha_2\delta$-1$^{-/-}$ mice, and $\alpha_2\delta$-1$^{-/-}$ DRG neurons exhibit lower calcium channel current density. Furthermore, a significantly smaller number of DRG neurons respond to the TRPM8 agonist menthol. After PSNL, $\alpha_2\delta$-1$^{-/-}$ mice show delayed mechanical hypersensitivity, which only develops at 11 d after surgery, whereas in wild-type littermates it is maximal at the earliest time point measured (3 d). There is no compensatory upregulation of $\alpha_2\delta$-2 or $\alpha_2\delta$-3 after PSNL in $\alpha_2\delta$-1$^{-/-}$ mice, and other transcripts, including neuropeptide Y and activating transcription factor-3, are upregulated normally. Furthermore, the ability of pregabalin to alleviate mechanical hypersensitivity is lost in PSNL $\alpha_2\delta$-1$^{-/-}$ mice. Thus, $\alpha_2\delta$-1 is essential for rapid development of mechanical hypersensitivity in a nerve injury model of neuropathic pain.

Introduction

Neuropathic pain can arise after disease or a lesion to the somatosensory system and is characterized by hyperalgesia, allodynia, dysesthesia, paresthesia, and often sensory loss (Costigan et al., 2009). The $\alpha_2\delta$-1 ligands gabapentin and pregabalin are effective in the treatment of a range of chronic neuropathic conditions (Moore et al., 2009, 2011). In several different animal models of neuropathic pain caused by peripheral nerve damage, there are many genes, including ion channels, whose expression is altered in injured dorsal root ganglion (DRG) neurons (Wang et al., 2002; Ji and Strichartz, 2004). In particular, there is an upregulation of the calcium channel auxiliary subunit $\alpha_2\delta$-1 (Newton et al., 2001; Wang et al., 2002). A corresponding increase in expression of $\alpha_2\delta$-1 protein is observed in both the affected ganglia and the spinal cord dorsal horn (Li et al., 2004; Bauer et al., 2009). The increase of $\alpha_2\delta$-1 in the spinal cord is the result of an elevation within the presynaptic terminals of the primary afferent neurons, rather than the intrinsic dorsal horn neurons (Bauer et al., 2009), and coincides with the onset of tactile allodynia (Li et al., 2004). In mice engineered to overexpress $\alpha_2\delta$-1, mimicking this aspect of sensory nerve damage, tactile allodynia is present in the absence of nerve damage (Li et al., 2006). Thus, there is a substantial body of evidence that the elevation of the $\alpha_2\delta$-1 subunit is relevant to the development of neuropathic pain, but it is unknown whether it is essential for this process.

One of the main effects of $\alpha_2\delta$ subunits on Ca_V1 and Ca_V2 calcium channels is to increase their functional expression, as

Received March 6, 2013; revised Aug. 8, 2013; accepted Aug. 27, 2013.

Author contributions: R.P., C.S.B., M.N.-R., A.H.D., and A.C.D. designed research; R.P., C.S.B., M.N.-R., W.M., L.F., K. Chaggar, K. Crews, and J.D.R. performed research; A.S. contributed unpublished reagents/analytic tools; R.P., C.S.B., M.N.-R., W.M., L.F., K. Crews, J.D.R., D.L.H.B., and A.C.D. analyzed data; R.P., C.S.B., M.N.-R., J.D.R., D.L.H.B., A.H.D., and A.C.D. wrote the paper.

This work was supported by the Medical Research Council United Kingdom Grants G0801756 and G0901758 and Wellcome Trust Programme Grant 098360/Z/12/Z to A.C.D., R.P. is supported by a Biotechnology and Biological Sciences Research Council studentship to A.H.D., A.S. is supported by the National Institutes of Health and National Heart, Lung, and Blood Institute. D.L.H.B. is supported by Senior Wellcome Trust Clinical Scientist Grant 095698/Z/11/Z. We thank Stuart Martin for genotyping; Dr. Peter McIntyre for TRPM8 cDNA; Dr. Armen Akopian for TRPV1 and TRPA1 cDNAs; Dr. Giandomenico Iannetti for loan of the infrared laser; and Dr. Lucy Bee and Dr. Michael Minett for technical assistance and advice.

The authors declare no competing financial interests.

*R.P., C.S.B., and M.N.-R. contributed equally to this work as first authors.

This article is freely available online through the *J Neurosci* Author Open Choice option.

Correspondence should be addressed to Dr. Annette C. Dolphin, Department of Neuroscience, Physiology and Pharmacology, Andrew Huxley Building, University College London, Gower Street, London, WC1E 6BT, United Kingdom. E-mail: a.dolphin@ucl.ac.uk.

C.S. Bauer's present address: Department of Biomedical Science, University of Sheffield, Sheffield, S10 2TN, United Kingdom.

DOI:10.1523/JNEUROSCI.1026-13.2013

evidenced by increased calcium current density, and increased channel protein at the plasma membrane (Gurnett et al., 1996; Qin et al., 1998; Wyatt et al., 1998; Barclay et al., 2001; Klugbauer et al., 2003; Cantí et al., 2005), and to increase transmitter release at presynaptic terminals (Hoppa et al., 2012).

In the present study, we have investigated the function of DRG and spinal neurons from mice with targeted disruption of the $\alpha_2\delta$-1 gene (Fuller-Bicer et al., 2009) to examine whether $\alpha_2\delta$-1 is involved in normal primary afferent function, in terms of thermal and mechanical sensitivity, using behavioral and electrophysiological approaches, and in their response to transient receptor potential (TRP) agonists. An important goal was to determine whether the $\alpha_2\delta$-1 subunit is essential for the initiation and maintenance of behavioral hypersensitivity after sensory nerve injury, to shed light on the molecular mechanism(s) responsible for neuropathic pain. Our main findings are that $\alpha_2\delta$-1$^{-/-}$ mice show a marked behavioral deficit in mechanical and cold sensitivity, but no change in thermal nociception threshold, together with a reduced sensitivity of their DRG neurons *in vitro* to TRPM8 agonists. The $\alpha_2\delta$-1$^{-/-}$ mice also exhibit a marked delay in the development of mechanical hypersensitivity and an insensitivity to pregabalin-mediated analgesia, in a nerve injury model of neuropathic pain. These results identify $\alpha_2\delta$-1 as a key component of the mechanical and cold somatosensory pathways.

Materials and Methods

Transgenic mice. Conventional $\alpha_2\delta$-1 knock-out C57BL/6 mice were obtained (Fuller-Bicer et al., 2009). All experiments were performed on male 9- to 12-week-old (unless otherwise stated) $\alpha_2\delta$-1$^{-/-}$ mice and $\alpha_2\delta$-1$^{+/+}$ littermates, obtained by breeding from heterozygotes. Mice were housed in groups of no more than 5 on a 12 h:12 h light dark cycle; food and water were available *ad libitum*. All experimental procedures were approved by the United Kingdom Home Office and followed the guidelines of the International Association for the Study of Pain (Zimmermann, 1983). For the *in vivo* studies, a total of 62 $\alpha_2\delta$-1$^{+/+}$ and 53 $\alpha_2\delta$-1$^{-/-}$ mice were used. All behavioral and *in vivo* electrophysiological characterizations were performed with the experimenter blind to the genotype and to drug administered.

Mechanical sensitivity. Mice were placed in isolation inside Perspex chambers on a wire mesh floor and allowed to acclimatize. Mechanical sensitivity was assessed using von Frey filaments (Touch-Test, North Coast Medical) providing forces of 0.07 g (0.69 mN), 0.16 g (1.57 mN), and 0.4 g (3.92 mN). Hairs were tested in ascending order and applied 10 times across left and right hindpaws. Hairs were applied until they buckled for 3–4 s; lifting, biting, and shaking were considered positive responses. Statistical differences between $\alpha_2\delta$-1$^{+/+}$ and $\alpha_2\delta$-1$^{-/-}$ groups were determined with the Mann–Whitney *U* test.

Cold sensitivity. Cold sensitivity was tested by applying a drop of acetone, using a modified 0.5 ml syringe with polythene tubing, to the left and right hindpaws. Acetone was applied 5 times, with at least 5 min recovery between applications. The initial response was disregarded as contact withdrawal. The duration of the delayed response (occurring 2–3 s later) was measured over the next 45 s. Flinching, licking, biting, and shaking were considered to be positive behaviors. Data are presented as mean response duration (in seconds). Statistical differences between $\alpha_2\delta$-1$^{+/+}$ and $\alpha_2\delta$ $^{-/-}$ groups were determined with an unpaired Student's *t* test.

Withdrawal threshold to noxious heat. Thermal thresholds were determined using an infrared Nd:YAP laser with a wavelength of 1.34 μm (Electronical Engineering). A He–Ne laser illuminated the area to be stimulated with a 3-mm-wide spot. The pulse time was 4 ms. Mice were lightly anesthetized and maintained on 0.8% v/v isofluorane (Baxter) delivered in a 3:2 ratio of nitrous oxide and oxygen. Body temperature was regulated using a homeothermic blanket (Harvard Apparatus). Reflexes were confirmed before each test by pinching between the toes. The laser was aligned across the footpads of the right hindpaw before applying an incremental thermal stimulus starting at 1 J. If no response was observed, the stimulus was increased by 0.5 J. Mice were allowed 3 min to recover between tests. Once a positive withdrawal was observed, the intensity was reduced by 0.25 J, to determine the approximate withdrawal threshold. Thresholds were confirmed by repeating the test on the left hindpaw. The cutoff was set at 3.5 J to prevent tissue damage. Statistical significances were determined using the Mann–Whitney *U* test.

In vivo electrophysiology. In vivo electrophysiology was conducted as previously described (Urch and Dickenson, 2003). Mice were anesthetized with intraperitoneal 2.4 g/kg urethane (Sigma) dissolved in 0.9% saline. Once mice were areflexic, a tracheotomy was performed before securing mice in a stereotaxic frame and performing a laminectomy to expose L3-L5 segments of the spinal cord. Extracellular recordings were made from deep dorsal horn lamina V/VI wide dynamic range (WDR) neurons, at depths of 350–700 μm (Watson et al., 2009), with receptive fields on the glabrous skin of the toes, using parylene-coated tungsten electrodes (A-M Systems). Seventeen neurons were characterized from 14 $\alpha_2\delta$-1$^{+/+}$ mice. Nineteen neurons were characterized from 15 $\alpha_2\delta$-1$^{-/-}$ mice.

Electrical stimulation of WDR neurons was delivered transcutaneously via needles inserted into the receptive field. A train of 16 electrical stimuli (2 ms pulses, 0.5 Hz) was applied at three times the threshold current for C fiber activation. Responses evoked by A (0–50 ms) and C (50–250 ms) fibers were separated and quantified on the basis of latency. Neuronal responses occurring after the C fiber latency band were classed as after discharge. The "input" (a theoretical nonpotentiated response) and the windup (potentiated response) were calculated as follows:

$$\text{Input} = (\text{action potentials evoked by first pulse}) \times \text{total number of pulses (16)}$$

$$\text{Wind-up} = (\text{total action potentials after 16 train stimulus}) - \text{input.}$$

The receptive field was also stimulated using a range of natural stimuli (dynamic brushing, von Frey filaments, Touch-Test, North Coast Medical): 0.4 g (3.92 mN), 1 g (9.81 mN), 4 g (39.23 mN), 8 g (78.45 mN), and 15 g (147.10 mN) and thermal stimuli at 42°C, 45°C, and 48°C applied over a period of 10 s per stimulus and the evoked response quantified. The thermal stimulus was applied with a constant water jet onto the center of the receptive field. The 35°C response was subtracted as it was considered to be predominantly the mechanical component of the stimulus. An acetone drop was applied as an innocuous cooling stimulus, preceded by a water drop to control for concomitant mechanical stimulation during application. Data were captured and analyzed by a Cambridge Electronic Design 1401 interface coupled to Spike 2 software with after stimulus time histogram and rate functions. Statistical differences in fiber threshold, electrical parameters, neuronal responses to cooling, and dynamic brush stimulation were determined using an unpaired Student's *t* test; Welch's correction was applied where appropriate. Linear regression was performed to examine the difference in the rate of windup after a log transformation. Differences in mechanical and thermal coding were determined using a two-way ANOVA, followed by a Bonferroni correction for multiple paired comparisons. Sphericity was tested with Mauchly's test; Greenhouse-Geiser corrections were used where required.

Partial sciatic nerve ligation (PSNL). Surgery was performed based on a method described previously (Selzer et al., 1990). Mice were maintained under 2% v/v isofluorane (Baxter) anesthesia delivered in a 3:2 ratio of nitrous oxide and oxygen. Under aseptic conditions, the left sciatic nerve was exposed through blunt dissection of the biceps femoris above the trifurcation of the nerve. Approximately half of the nerve was ligated with a nonabsorbable 7-0 braided silk thread (Ethicon, VetTech). The surrounding muscle was closed with absorbable 6-0 vicryl sutures (Ethicon, VetTech), and the skin with surgical wound clips. Sham surgery was performed in wild-type mice in an identical manner omitting the nerve

ligation step. After surgery, the mice were allowed to recover. Foot posture and general behavior of the operated mice were monitored throughout the postoperative period. Two mice with impaired motor activity were omitted from this study. Mechanical and cold hypersensitivity were tested on postoperative days 3, 7, 9, 11, and 14. Mechanical hypersensitivity was compared with the Kruskal–Wallis test, and paired comparisons were made with Dunn's *post hoc* test followed by a Bonferroni correction. Cold hypersensitivity was compared with a two-way repeated-measures ANOVA, followed by a Bonferroni correction for multiple paired comparisons. Behavioral pharmacology was performed 14 d after injury, with the observer blinded to the treatment. $\alpha_2\delta$-1$^{+/+}$ and $\alpha_2\delta$-1$^{-/-}$ mice were intraperitoneally administered either vehicle (0.9% saline) or 10 mg/kg pregabalin (gift from Pfizer) in a volume of 5 ml/kg. Mechanical hypersensitivity was tested at 30, 60, and 90 min after dosing. Differences to predrug withdrawal frequencies were compared with the Friedman test, followed by a Wilcoxon *post hoc* and Bonferroni correction for paired comparisons. Differences between vehicle and pregabalin groups were compared with the Mann–Whitney test.

DRG cultures. DRGs were removed from the entire spine of $\alpha_2\delta$-1$^{+/+}$ and $\alpha_2\delta$-1$^{-/-}$ mice at age 10 weeks, according to Schedule 1 guidelines (Home Office Animals Scientific Procedures Act 1986, United Kingdom). Cell cultures were obtained after enzymatic and mechanical dispersal as described previously (Hendrich et al., 2008). For Ca^{2+}-imaging experiments, DRGs were incubated in Hank's basal salt solution containing 1000 U/ml DNase (Invitrogen), 5 mg/ml dispase (Invitrogen), and 2 mg/ml collagenase type 1A (Sigma) for 18 min at 37°C. The partially digested ganglia were then washed and triturated in growth medium (DMEM/F12 with 10% FBS), 2 mM GlutaMAX (Invitrogen), 100 U/ml penicillin, 100 μg/ml streptomycin, and 6 g/L glucose and plated on coverslips coated with poly-L-lysine (Sigma) and laminin (Sigma). For electrophysiological experiments, DRGs were incubated in Hank's basal salt solution containing 100 U/ml DNase, 5 mg/ml dispase, and 2 mg/ml collagenase type 1A for 30 min at 37°C, the growth medium had no glucose added, and laminin was not used as a substrate.

In vitro electrophysiology. Calcium channel currents in DRG neurons were investigated by whole-cell patch-clamp recording (after 1 DIV). The patch pipette solution contained in mM the following: 140 Cs-aspartate, 5 EGTA, 2 $MgCl_2$, 0.1 $CaCl_2$, 2 ATP, 20 HEPES, pH 7.2, 310 mOsm with sucrose. The external solution for recording Ba^{2+} currents contained in mM as follows: 150 tetraethyl-ammonium Br, 3 KCl, 1.0 $NaHCO_3$, 1.0 $MgCl_2$, 10 HEPES, 4 glucose, 2 $BaCl_2$, 0.001 TTX, pH 7.4, 320 mOsm with sucrose. Measurements were made at 30 ms after the start of the voltage step. Analysis was performed as previously described (Cantí et al., 2005). Mean I-V relationships were fitted with a modified Boltzmann equation as follows:

$$I = G_{max}(V - V_{rev})/(1 + \exp[-(V - V_{50,act})/k])$$

where G_{max} is the maximum conductance, V_{rev} is the reversal potential, k is the slope factor, and $V_{50,act}$ is the voltage for 50% current activation. In experiments in which N-type calcium currents were blocked, cells were preincubated for 15 min in DMEM/F12 (0% FBS) with ω-conotoxin GVIA (1 μM), and recorded in the external solution in the presence of the toxin. I-V relationships recorded in cells from $\alpha_2\delta$-1$^{+/+}$ and $\alpha_2\delta$-1$^{-/-}$ mice, with or without ω-conotoxin GVIA, were compared with two-way ANOVA, followed by *post hoc* pairwise comparison with Tukey Honest Significant Differences test.

Intracellular calcium imaging. Cultures of DRG neurons (1 DIV) were loaded with 5 μM fura-2 AM in growth medium for 15 min and then washed in external solution (145 mM NaCl, 2 mM KCl, 5 mM $NaHCO_3$, 2.5 mM $CaCl_2$, 1 mM $MgCl_2$, 10 mM HEPES, 10 mM glucose, pH 7.4, adjusted with NaOH) for 20 min at 37°C. Imaging was performed using an Axiovert 200M microscope (Zeiss) with an ORCA-ER camera (Hamamatsu) at 30°C. Images were captured sequentially (0.5 Hz acquisition rate per paired image) at 340 and 380 nm excitation and 510 nm emission, and the ratio (340/380 nm) was calculated offline for subsequent analysis using Volocity 4 software (Improvision). After a 30 s baseline acquisition, agonists were applied in external solution sequentially in two different experimental series. In the first series, the application order was as follows: 100 μM allyl isothiocyanate (mustard oil [MO], 500 mM stock in DMSO, Sigma) for 20 s, followed by 500 μM (1*R*, 2*S*, 5*R*)-(−)-menthol (ME, 500 mM stock in EtOH, Sigma) for 30 s, followed by 1 μM capsaicin (C or CAPS, 10 mM stock in EtOH, Sigma) for 10 s. In the second series, the application order was as follows: 250 μM ME for 30 s, followed by 100 μM trans-cinnamaldehyde (CA, 500 mM in EtOH, Sigma) for 60 s, followed by 1 μM CAPS for 5 s. Agonist applications were separated by 90 s of washing in external solution. In a separate set of experiments, cells were stimulated with 20 μM WS-12 (20 mM stock in DMSO, Sigma) for 30 s followed by 250 μM ME for 30 s with a 3 min washing period between agonist applications. The elevation of intracellular Ca^{2+} in DRG neurons induced by a 10 s high K^+ application (85 mM NaCl, 60 mM KCl, 5 mM $NaHCO_3$, 2.5 mM $CaCl_2$, 1 mM $MgCl_2$, 10 mM HEPES, 10 mM glucose, pH 7.4, adjusted with NaOH) 90 s after the last agonist application was used as an indicator of cell viability. Cells not responding to high K^+ were excluded from the analysis. To quantify, the number of responses for each agonist per coverslip were counted and normalized to the number of cells responding to K^+ (100%). Responses to ME and CAPS were pooled from experiments using both agonist sequences 1 and 2 (see above). Responses to MO (sequence 1) and CA (sequence 2) were analyzed separately. In total, 982 $\alpha_2\delta$-1$^{+/+}$ and 1151 $\alpha_2\delta$-1$^{-/-}$ cells were analyzed. Peak ratio amplitudes were determined relative to a normalized fluorescence ratio (R = 1.0) measured before agonist application.

Quantitative PCR. DRGs from the lumbar region 3–5 (L3-L5) were dissected as described previously (Rigaud et al., 2008), from nine sham $\alpha_2\delta$-1$^{+/+}$, 7 PSNL $\alpha_2\delta$-1$^{+/+}$ and 7 PSNL $\alpha_2\delta$-1$^{-/-}$ mice, 14 d after surgery from both the ipsilateral and contralateral sides. DRGs were also taken from three $\alpha_2\delta$-1$^{+/+}$ and three $\alpha_2\delta$-1$^{-/-}$ naive mice in the same manner. For quantitative PCR (Q-PCR) and immunoblot assays, the methods used were essentially as described previously (Bauer et al., 2009). Briefly, RNA was extracted from pooled L3-L5 pulverized frozen DRGs using RNeasy columns (QIAGEN), including an on-column DNase step. Reverse transcription was performed using Superscript III reverse transcriptase (Invitrogen) and random hexamer primers (Promega). Q-PCR of sample duplicates was performed with an Applied Biosystems 7500/7500 Fast Real-Time PCR system. The following TaqMan assays with TaqMan Gene Expression Master Mix were used according to the manufacturer's protocol (gene name: assay ID): *GAPDH:* Mm99999915_g1; *CACNA2D1:* Mm00486607_m1; *CACNA2D2:* Mm00457825_m1; *CACNA2D3:* Mm00486613_m1; *ATF3:* Mm00476032_m1; *TRPV1:* Mm01246302_m1; *TRPM8:* Mm01299593_m1; *TRPA1*: Mm01227437_m1; *PIEZO2*: Mm01265861_m1; and *CACNB3*: Mm00432244_m1.

The comparative C_T ($\Delta\Delta C_T$) method was used for relative quantification of fold differences (given as the mean ± SEM) of mRNA levels between the ipsilateral and contralateral side from mice that had undergone surgery. For this, data were first normalized for expression of GAPDH mRNA by calculating ΔC_T. Statistical significance between $\alpha_2\delta$-1, $\alpha_2\delta$-2, $\alpha_2\delta$-3, and activating transcription factor 3 (ATF3) and $Ca_V\beta$3 mRNA levels in sham and PSNL or $\alpha_2\delta$-1$^{+/+}$ and $\alpha_2\delta$-1$^{-/-}$ mice was determined by a one-way ANOVA test with Bonferroni's *post hoc* test. Statistical significance of differences for TRPM8, TRPA1, TRPV1, and Piezo2 mRNA levels between $\alpha_2\delta$-1$^{+/+}$ and $\alpha_2\delta$-1$^{-/-}$ mice was determined by a one-sample *t* test (compared with a theoretical value of 1) and by unpaired Student's *t* test. The $\Delta\Delta C_T$ method was also used for relative quantitation of fold differences of TRP channel mRNA levels from naive mice. The mean value of the left and right DRG samples of each $\alpha_2\delta$-1$^{-/-}$ and $^{+/+}$ mouse was normalized to the mean value of the $\alpha_2\delta$-1$^{+/+}$ samples, and statistical analysis was determined by Student's unpaired *t* test.

Transfection of tsA-201 cells. Cells were transfected with cDNA for N-terminal c-myc tagged mouse TRPM8, TRPV1, or TRPA1, together with either $\alpha_2\delta$-1 or β1b, at a ratio of 1:1 using FuGENE according to the manufacturer's protocol (Promega). Myc-TRPM8 was in pcDNA5/FRT, myc-TRPV1 and myc-TRPA1 were in pCMV-myc, and $\alpha_2\delta$-1 and β1b were in pMT2.

Immunoblotting. Proteins were extracted from DRG neurons, brain, and skeletal muscle from hind leg, using a buffer of PBS with 1 mM EDTA and 1 μM DTT in the presence of protease inhibitors (complete EDTA free, Roche

Diagnostics) by homogenization, followed by incubation with 0.2% SDS and 1% Igepal for 40 min on ice. Synaptosomes were prepared from whole brain and spinal cord as previously described (Kato et al., 2007) and solubilized in 50 mM Tris, pH 8, 150 mM NaCl, 1% Igepal, 0.5% Na deoxycholate, 0.1% SDS (Ferron et al., 2008). DRG samples were precleared of IgGs by incubation with Protein-G-agarose beads (Santa Cruz Biotechnology) for 1 h at 4°C, and then deglycosylated with 0.1 U/μl endoglycosidase F (PNGase F, Roche) for 1.5 h at 37°C. After centrifugation (20 min at 13,000 × g at 4°C), samples were loaded onto a 3–8% NuPage Tris/acetate gel (Invitrogen) and proteins were separated by SDS-PAGE. Proteins were transferred to PVDF membranes (Bio-Rad) and, after blocking (500 mM NaCl, 10 mM Tris, pH 7.4, with 3% BSA and 0.5% Igepal), blots were probed with the mouse monoclonal anti-dihydropyridine receptor (α_2-1 subunit) antibody (α_2-1 Ab, 1:2000, Sigma) or in-house $Ca_V2.2$ polyclonal Ab (1:500; Raghib et al., 2001) or with the mouse monoclonal anti-GAPDH Ab (1:25,000, Ambion) at 4°C overnight. Similarly, for the detection of Myc-tagged TRP channels, in transiently transfected tsA-201 cells, 60 μg of WCL was separated by SDS-PAGE, transferred to PVDF membrane, and probed with the mouse monoclonal anti-Myc Ab (1:1000, Santa Cruz Biotechnology), or with the mouse monoclonal anti-GAPDH Ab (1:25,000, Ambion) for 1 h. The protein–Ab complexes were then labeled with a HRP-conjugated secondary Ab (1:2000, Sigma) for 1 h at room temperature (RT). Bands were detected using the enhanced ECL Plus reagent (GE Healthcare) visualized with a Typhoon 9410 scanner (GE Healthcare). Densitometric quantification of immunoblot bands was performed with ImageQuant software (GE Healthcare) and normalized to the respective GAPDH loading control.

Immunohistochemistry. L3-L5 DRGs were removed and postfixed for 2 h in 0.1 M phosphate buffer (PB), pH 7.4, with 4% PFA, followed by incubation in PB with 15% sucrose and 0.05% NaN_3 overnight, and finally frozen in optimal cutting temperature (OCT) compound (VWR) before sectioning at 10 μm using a cryostat. Immunofluorescence labeling for $\alpha_2\delta$-1 (mouse monoclonal anti-dihydropyridine receptor Ab (α_2-1 subunit), 1:100, Sigma) and neuropeptide Y (NPY, rabbit polyclonal Ab, 1:1000,Abcam) was performed as described previously (Bauer et al., 2009) with the following alterations. After heat-induced epitope retrieval (10 mM citrate buffer, pH 6.0, 0.05% Tween 20, 95°C for 10 min), the sections were incubated in 1% Triton X-100 in PBS for 1 h at RT and blocking with 10% goat serum in PBS containing 0.1% Triton X-100 for >1 h at RT; and to reduce the background signal resulting from the use of a mouse Ab on mouse tissue, endogenous IgGs were blocked by incubation with the unconjugated goat Fab anti-mouse IgG (H+L) (0.1 mg/ml in PBS, Jackson ImmunoResearch Laboratories) for 1 h at RT. Primary Abs were applied for 2 or 3 d at 4°C. After extensive washes, the samples were incubated with biotin-conjugated goat Fab fragment anti mouse for 2 h at 4°C (1:500, Jackson ImmunoResearch Laboratories), followed by washes and streptavidin-AlexaFluor-488 and anti-rabbit-AlexaFluor-594 for 1 h at RT (both at 1:500, Invitrogen). Nuclei were stained with DAPI (500 nM) before mounting in Vectashield (Vector Laboratories). Staining with the neuronal markers peripherin (mouse monoclonal Ab, 1:500, Sigma) and neurofilament 200 (NF200, rabbit polyclonal Ab, 1:200, Sigma) was performed on sections of L4 DRGs, which were either washed with PB, followed by incubation in PB with 15% sucrose and 0.05% NaN_3 overnight, and finally frozen in OCT or immediately frozen in OCT before being sectioned to a thickness of 10 μm. After fixation for 7 min with 4% PFA in PBS, sections were blocked in 10% goat serum in the presence of 0.3% Triton X-100 for at least 2 h. Primary Abs were applied at 4°C overnight in blocking solution. Sections were then washed with PBS + 0.3% Triton X-100, incubated with biotin-conjugated goat anti-rabbit IgG (1:500, Sigma) in blocking buffer for 2 h at RT, washed with PBS + 0.3% Triton X-100 before incubation with anti-mouse FITC (1:500, Sigma) and streptavidin-AlexaFluor-594 (1:500, Invitrogen) for 1 h. After washing, sections were stained with DAPI (500 nM) before the samples were mounted in VectaShield (Vector Laboratories).

Image acquisition and analysis. Immunofluorescence labeling of peripherin and NF200 was detected with a Zeiss Axiovert 200M microscope. Images of 14 sections from four $\alpha_2\delta$-1$^{+/+}$ and 13 sections from three $\alpha_2\delta$-1$^{-/-}$ mice were analyzed. For this, the percentage of cells positive for NF200, peripherin, or both neuronal markers was calculated per section. Only intact cells with a clearly visible nucleus were counted. Statistical analysis (Student's unpaired *t* test) was performed after arcsin transformation of the data. Immunostaining for $\alpha_2\delta$-1 and NPY was visualized using an LSM 510 Meta (Zeiss) confocal microscope. To quantify the NPY staining, images were acquired with constant settings from at least 8 sections (with a minimum distance between sections from the same DRG of 20 μm) from at least three mice. Only cells with a visible nucleus were used for analysis. Images were converted to gray levels using ImageJ software (http://rsb.info.nih.gov/ij) and a threshold determined by using images taken from negative control sections were the primary Ab was omitted during the immunohistochemical procedure. Cells with a gray level intensity higher than the threshold were counted as NPY-positive cells, and the number of NPY-positive cells per section was established. Statistical significance was determined with Student's unpaired *t* test.

Immunohistochemistry on skin. Skin biopsies were taken from the left hindpaw of 4 $\alpha_2\delta$-1$^{+/+}$ and 4 $\alpha_2\delta$-1$^{-/-}$ mice. Skin samples were fixed using 4% PFA in 0.1 M PB and then preserved in 15% sucrose before being blocked and further processed into 14 μm sections. Nerve fibers were stained using rabbit anti-PGP 9.5 Ab (1:2000, Ultraclone) and Cy3 anti-rabbit Ab (1:500, Jackson ImmunoResearch Laboratories). Images were acquired using a Zeiss LSM 710 upright confocal microscope, with an EC Plan-Neofluar objective at 40× magnification. The 2 μm interval images were acquired for each section, and the maximum intensity projection tool was used. The samples were processed and analyzed blind with respect to the genotype. The samples were analyzed by the same investigator (J.D.R.), and analysis was performed as explained previously (Ramirez et al., 2012). Briefly, PGP9.5-positive nerve fibers crossing the basal membrane were counted, and a measurement of the length of the sample was then obtained. Intraepidermal nerve fiber density counts are given in number of fibers per millimeter length of epidermis.

Statistics. Statistical analyses were performed using GraphPad Prism 4.03, SPSS version 20 (IBM) or R (R Development Core Team, 2012). For all statistical tests: $^{***}p < 0.001$, $^{**}p < 0.01$, $^{*}p < 0.05$, not significant $p > 0.05$, except where actual *p* values given.

Results

$\alpha_2\delta$-1 protein is not expressed in tissue from $\alpha_2\delta$-1 knock-out mice

We confirmed that $\alpha_2\delta$-1 protein was absent from brain and skeletal muscle of $\alpha_2\delta$-1$^{-/-}$ mice (Fig. 1*A*). In L4 + L5 DRGs, $\alpha_2\delta$-1 was present in +/+ mice, and absent from $\alpha_2\delta$-1$^{-/-}$ littermates, a result confirmed by deglycosylation of the samples, where the expected reduction in MW of the $\alpha_2\delta$-1-immunoreactive band was seen in +/+ DRGs from ~150 kDa to ~105 kDa (Fig. 1*B*, lanes 2 and 4). In brain synaptosomes from $\alpha_2\delta$-1$^{-/-}$ mice at 10 weeks old, we also found a reduced level of $Ca_V2.2$ protein compared with littermate $\alpha_2\delta$-1$^{+/+}$ tissue (a 25.4 ± 5.8% reduction from four independent experiments, $p = 0.022$), although this was not evident in whole brain (Fig. 1*C*). This result is indicative of reduced presynaptic levels of this channel in the absence of $\alpha_2\delta$-1. A similar result was obtained in spinal cord synaptosomes, in which there was a reduction of $Ca_V2.2$ protein in $\alpha_2\delta$-1$^{-/-}$ compared with $\alpha_2\delta$-1$^{+/+}$ tissue by 56.8 ± 9.9% (from four independent experiments, $p = 0.0107$; Fig. 1*D*).

Deficits in behavioral responses to mechanical and innocuous cooling stimuli in $\alpha_2\delta$-1$^{-/-}$ mice

$\alpha_2\delta$-1$^{-/-}$ mice and wild-type littermate controls were initially examined for behavioral differences in mechanical, cold, and thermal sensitivity. Mechanical sensitivity was tested using von Frey filaments, which were applied across the hindpaws. Significantly fewer withdrawals were observed in $\alpha_2\delta$-1$^{-/-}$ mice in response to 0.16 g and 0.4 g filaments but not 0.07 g, the lowest weight tested (Fig. 2*A*). The $\alpha_2\delta$-1$^{-/-}$ mice also displayed significantly fewer nocifensive behaviors in response to acetone application to the hindpaws as an evaporative cooling stimulus (Fig. 2*B*). Nociceptive reflexes to thermal stimulation were conducted

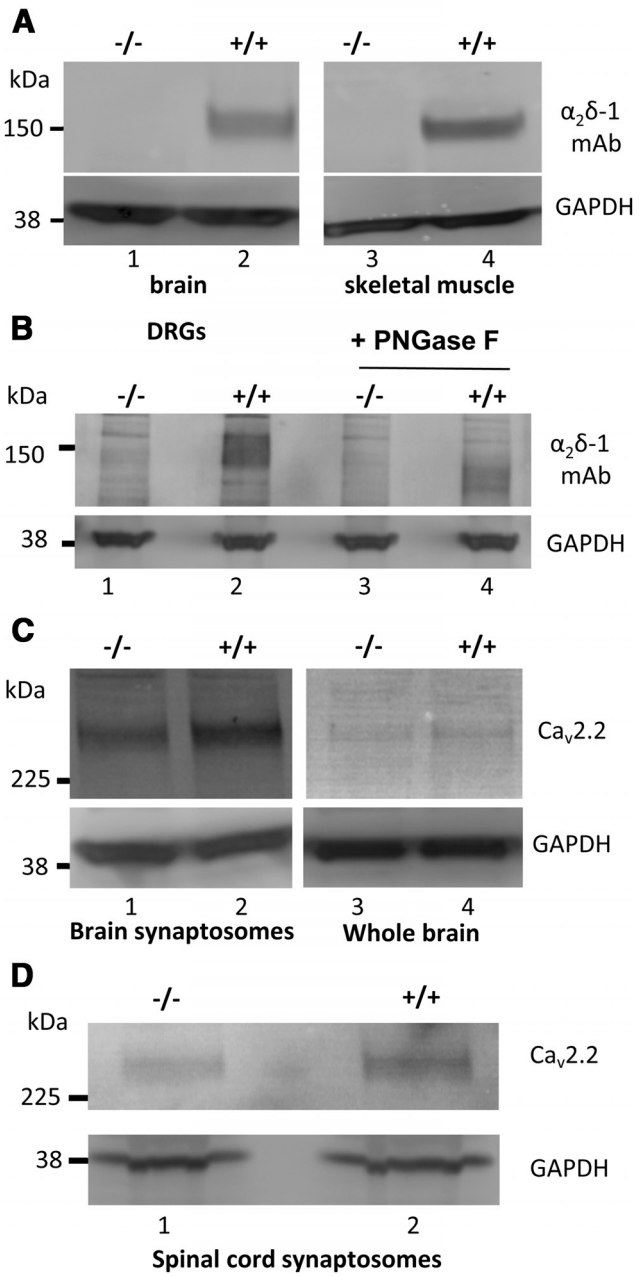

Figure 1. Immunoblotting for $\alpha_2\delta$-1 and $Ca_V2.2$ in $+/+$ and $-/-$ mice tissues. ***A***, Comparison of $\alpha_2\delta$-1 levels in brain (left panel) and skeletal muscle (right panel) in $\alpha_2\delta$-1$^{-/-}$ (lanes 1, 3) and $\alpha_2\delta$-1$^{+/+}$ (lanes 2, 4). A total of 20 μg of protein was loaded/lane. No $\alpha_2\delta$-1 is observed in $\alpha_2\delta$-1$^{-/-}$ mice. Immunoblot for GAPDH (bottom panel) provides the loading control. ***B***, $\alpha_2\delta$-1 levels in DRGs from $\alpha_2\delta$-1$^{-/-}$ (lanes 1, 3) and $\alpha_2\delta$-1$^{+/+}$ (lanes 2, 4) mice. Material (30 μg of protein/lane) in lanes 3 and 4 has been deglycosylated with PNGase F, showing the characteristic decrease in MW of $\alpha_2\delta$-1 from ~150 kDa (lane 2) to ~105 kDa (lane 4). No corresponding bands are observed in $\alpha_2\delta$-1$^{-/-}$ ganglia. GAPDH (bottom) provides a loading control. Data are representative of $n = 3$ experiments. ***C***, $Ca_V2.2$ levels in cerebral synaptosomes (left) and brain WCL (right) from $\alpha_2\delta$-1$^{-/-}$ (lanes 1, 3) and $\alpha_2\delta$-1$^{+/+}$ (lanes 2, 4) mice. GAPDH (bottom) provides a loading control for $Ca_V2.2$ quantification. Data are representative of $n = 4$ experiments. ***D***, $Ca_V2.2$ levels in spinal cord synaptosomes (top) from $\alpha_2\delta$-1$^{-/-}$ (lane 1) and $\alpha_2\delta$-1$^{+/+}$ (lane 2) mice. GAPDH (bottom) provides a loading control for $Ca_V2.2$ quantification. Data are representative of $n = 4$ experiments.

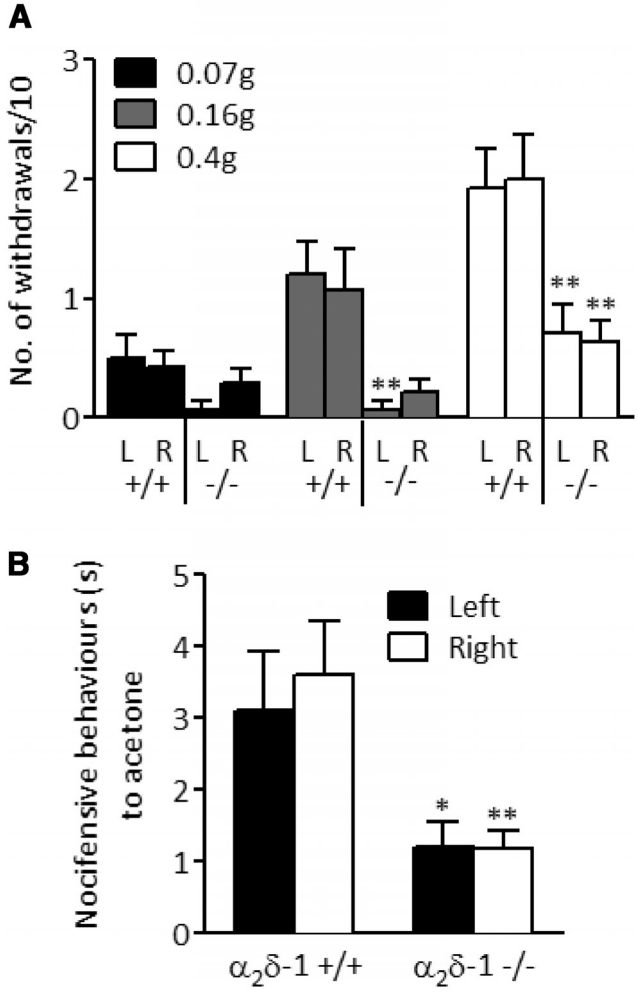

Figure 2. Behavioral responses of $\alpha_2\delta$-1$^{+/+}$ and $\alpha_2\delta$-1$^{-/-}$ mice to mechanical, cooling, and thermal stimuli applied to the hindpaws. ***A***, Withdrawal frequency to punctate mechanical stimulation applied using von Frey filaments. L, Left hindpaw; R, right hindpaw. $n = 14$. ***B***, Duration of nocifensive behaviors in response to acetone application (unpaired Student's *t* test with Welch's correction, $n = 12$). No significant differences were observed between left and right responses within genotypes. *$p < 0.05$, significant differences between respective paws between genotypes (Mann–Whitney *U* test). **$p < 0.01$, significant differences between respective paws between genotypes (Mann–Whitney *U* test). Data represent mean ± SEM.

in lightly anesthetized mice, using infrared laser stimulation, which has been previously demonstrated to stimulate Aδ and C fibers selectively (Sikandar et al., 2013). There was no significant difference in noxious thermal withdrawal thresholds, as determined by infrared laser stimulation, between $\alpha_2\delta$-1$^{+/+}$ mice (1.60 ± 0.19 J, $n = 10$) and $\alpha_2\delta$-1$^{-/-}$ mice (1.89 ± 0.20 J, $n = 9$) ($p = 0.319$, Mann–Whitney *U* test).

Deficits in sensory coding of lamina V/VI dorsal horn neurons

In vivo electrophysiology was performed to assess the impact of $\alpha_2\delta$-1 deletion on the spinal processing of a range of thermal and mechanical stimuli. All neurons characterized had receptive fields on the glabrous skin of the hind toes and were identified as WDR by confirming responses to light brushing, noxious punctate mechanical stimulation, and thermal stimulation. Neurons were characterized from similar depths, corresponding to deep dorsal horn laminae ($\alpha_2\delta$-1$^{+/+}$, 516 ± 26 μm; $\alpha_2\delta$-1$^{-/-}$, 542 ± 25 μm).

Deep dorsal horn neurons responded to mechanical and thermal stimulation in an intensity-dependent manner. The reduced behavioral response to punctate mechanical stimulation in $\alpha_2\delta$-1$^{-/-}$ mice (Fig. 2*A*) is corroborated by a deficit in mechanical

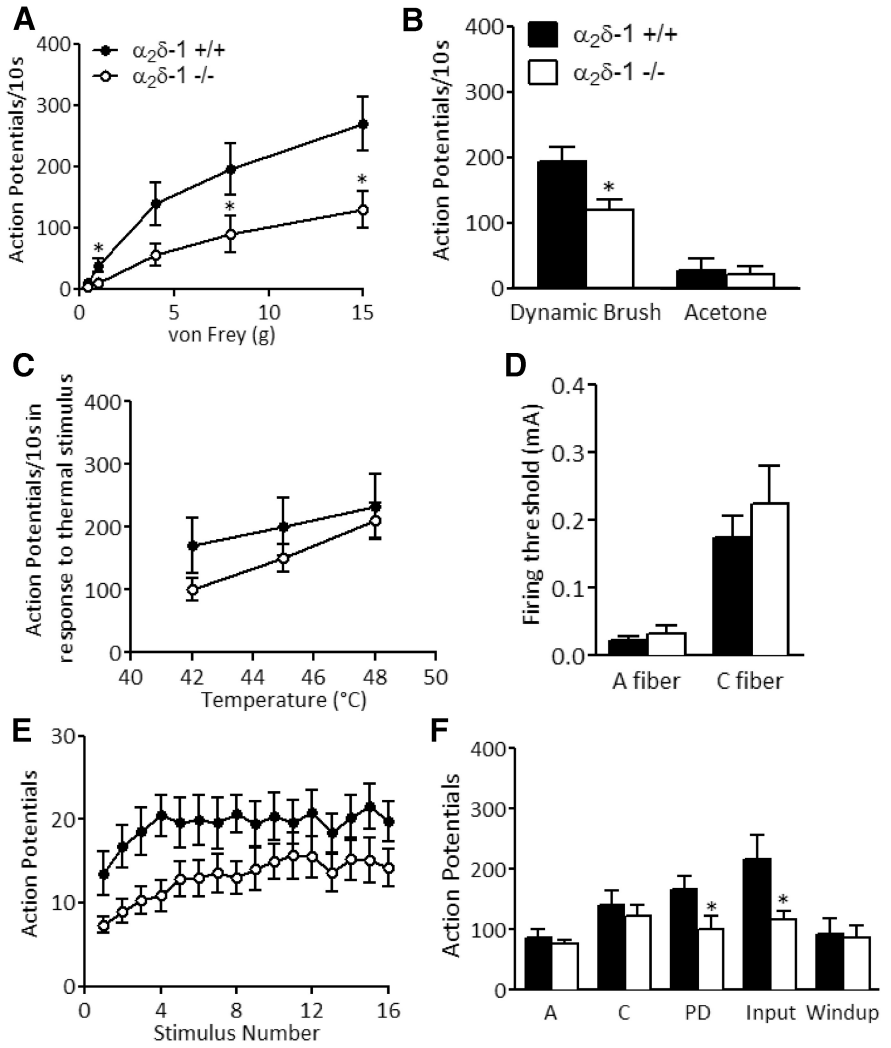

Figure 3. Comparison of responses to mechanical, thermal, and electrical stimulation of deep dorsal horn lamina V/VI wide dynamic range neurons in $\alpha_2\delta$-1$^{+/+}$ and $\alpha_2\delta$-1$^{-/-}$ mice. ***A***, Evoked neuronal responses to punctate mechanical stimulation (two-way ANOVA, $p < 0.05$, followed by Bonferroni *post hoc*). ***B***, Left, Evoked neuronal responses to dynamic brush stimulation (unpaired Student's *t* test, $p < 0.05$). Right, Cooling-evoked neuronal responses (unpaired Student's *t* test). ***C***, Thermally evoked neuronal responses (two-way ANOVA, $p > 0.05$). ***D***, Electrical thresholds for activation of A and C fibers ($p > 0.05$, unpaired Student's *t* test). ***E***, Windup of deep dorsal horn neurons (16 stimuli, 0.5 Hz, 2 ms pulse), expressed as mean number of action potentials per stimulus number. ***F***, Total action potentials evoked in response to repeated electrical stimulation, separated according to latency: A: 0–50 ms, C: 50–250 ms, PD (post-discharge) >250 ms. Input and windup were calculated as described in Materials and Methods. *n* for +/+ = 17, *n* for −/− = 19. *$p < 0.05$ (unpaired Student's *t* test). Data represent mean ± SEM.

coding of lamina V/VI neurons with significantly reduced neuronal responses to 1, 8, and 15 g stimulation (Fig. 3*A*). In addition, neuronal responses to dynamic brush stimulation were also attenuated (Fig. 3*B*, left). In contrast to the behavioral response to acetone-induced cooling (Fig. 2*B*), deep dorsal horn neuronal responses in $\alpha_2\delta$-1$^{-/-}$ mice were not different from the $\alpha_2\delta$-1$^{+/+}$ controls (Fig. 3*B*, right). However, only 5 of 17 $\alpha_2\delta$-1$^{+/+}$ neurons and 5 of 19 $\alpha_2\delta$-1$^{-/-}$ neurons were responsive to cooling, consistent with previous reports of minimal cold sensitivity in this temperature range in rat deep dorsal horn neurons (Khasabov et al., 2001). No significant difference in thermal coding of lamina V/VI neurons was observed in $\alpha_2\delta$-1$^{-/-}$ mice (Fig. 3*C*), supporting our earlier observation of unaltered thermal withdrawal thresholds.

Electrical thresholds for activation of A and C fibers were indistinguishable between the genotypes (Fig. 3*D*). After repeated suprathreshold electrical stimulation of the receptive field (16 stimuli, 2 ms pulse, 0.5 Hz), the cumulative total of neuronal events evoked by A and C fiber stimulation was not affected in $\alpha_2\delta$-1$^{-/-}$ mice (Fig. 3*E*,*F*). Lamina V/VI neurons from $\alpha_2\delta$-1$^{+/+}$ and $\alpha_2\delta$-1$^{-/-}$ exhibited a similar rate of windup (Fig. 3*E*), in addition to a similar total windup (Fig. 3*F*). Windup is an NMDA-dependent phenomenon where dorsal horn neurons become hyperexcitable after repeated C fiber stimulation (Dickenson and Sullivan, 1987). However, "input," the nonpotentiated response, more indicative of presynaptic events, and the post-discharge, a property of spinal neurons, were significantly decreased in $\alpha_2\delta$-1$^{-/-}$ mice (Fig. 3*F*).

DRG neurons from $\alpha_2\delta$-1$^{+/+}$ and $\alpha_2\delta$-1$^{-/-}$ mice are not different in their expression of neurofilaments

DRG neurons are highly heterogeneous in their sensory properties and physiological function. They can be grouped into distinct subpopulations by many different criteria, for example, according to their differential expression of neurofilaments, a component of the cytoskeleton (Goldstein et al., 1991; Ruscheweyh et al., 2007). We used immunohistochemical methods to visualize the expression of the intermediate filaments peripherin and NF200 in DRG sections from $\alpha_2\delta$-1$^{+/+}$ and $\alpha_2\delta$-1$^{-/-}$ mice. Peripherin is expressed in nonmyelinated nociceptive C fibers, whereas NF200 is expressed in myelinated nociceptive and non-nociceptive A fibers (Ruscheweyh et al., 2007). The majority of cell bodies in $\alpha_2\delta$-1$^{-/-}$ L4 DRG sections showed positive staining for either peripherin or NF200, with a small number of cells showing staining for both intermediate filaments (Fig. 4*A*). The proportion of cells that were peripherin-positive (~60%), NF200-positive (~40%), or positive for both neurofilaments (~4%) was not significantly different in L4 DRG sections from $\alpha_2\delta$-1$^{+/+}$ compared with $\alpha_2\delta$-1$^{-/-}$ mice (Fig. 4*B*), and is similar to the proportional staining reported by others for mice (Quick et al., 2012). These results show that the proportion of unmyelinated C-fibers and myelinated A-fibers is unchanged by the ablation of $\alpha_2\delta$-1.

Normal numbers of sensory neuron axons in the skin of $\alpha_2\delta$-1$^{-/-}$ mice

We examined the peripheral innervation of sensory fibers and observed no difference in density of PGP 9.5-positive axons crossing the dermal–epidermal boundary, in agreement with the lack of gross differences between DRG neurons in $\alpha_2\delta$-1$^{+/+}$ and $\alpha_2\delta$-1$^{-/-}$ mice. For $\alpha_2\delta$-1$^{+/+}$ mice, there were 30.4 ± 1.7 axons/mm of epidermis; and for $\alpha_2\delta$-1$^{-/-}$ mice, there were 28.6 ± 5.4 axons/mm, crossing the dermal–epidermal boundary ($n = 4$ mice, 3 sections per mouse; Fig. 4*C*,*D*).

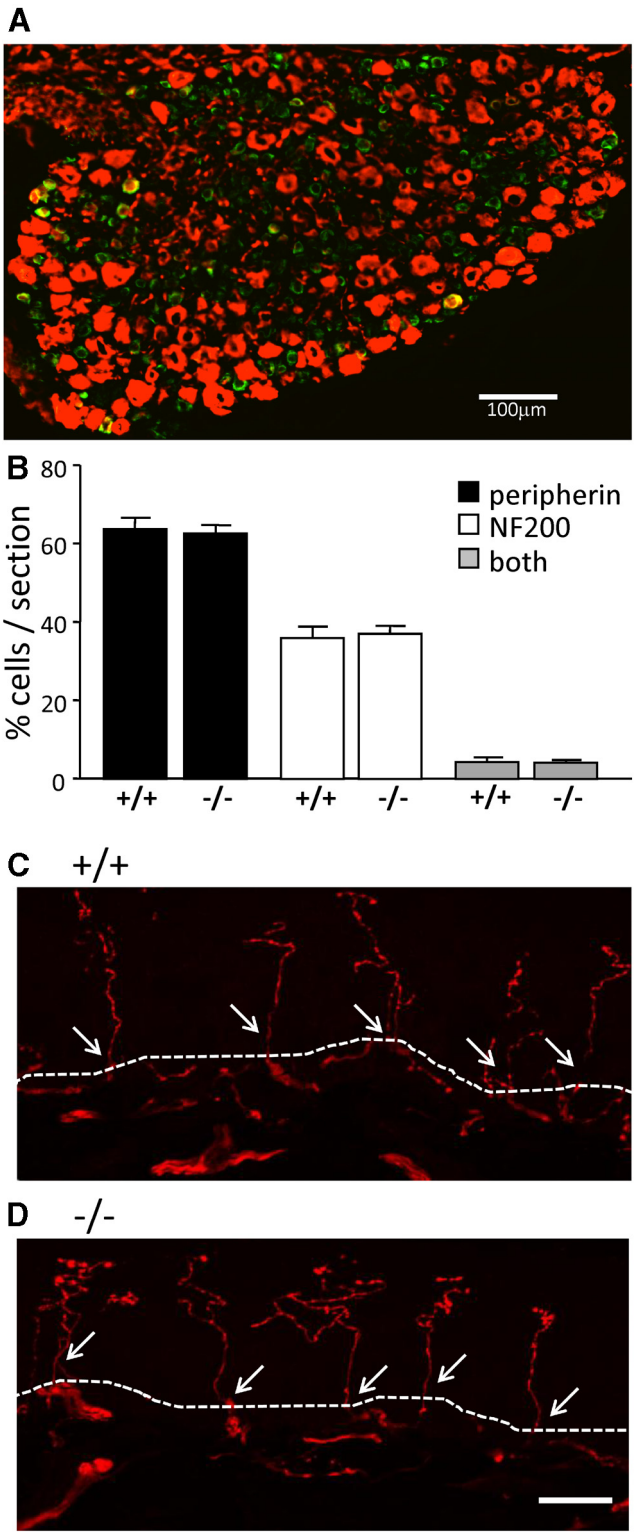

Figure 4. Sensory neuronal subpopulations and terminals in the skin are not different between $\alpha_2\delta$-1$^{+/+}$ and $\alpha_2\delta$-1$^{-/-}$ DRGs. ***A***, Representative double immunofluorescence staining for the neuronal intermediate filaments peripherin (green) and NF200 (red) in an L4 DRG section from an $\alpha_2\delta$-1$^{-/-}$ mouse. The majority of cell bodies are positive for peripherin or NF200, with a small number of cells showing staining for both intermediate filament types (yellow). ***B***, Quantification of peripherin (black bars), NF200 (white bars), and staining for both intermediate filament types (both, gray) in L4 DRGs from $\alpha_2\delta$-1$^{+/+}$ and $\alpha_2\delta$-1$^{-/-}$ mice, shown as percentage of cells stained per section. Data represent mean ± SEM. Statistical analysis was as follows: unpaired Student's *t* test comparing $n = 14$ +/+ with $n = 13$ −/− sections from four mice, respectively; $p = 0.727$ for peripherin, $p = 0.073$ for NF200, $p = 0.70$ for both. ***C***, ***D***, Images of PGP 9.5-positive axons crossing the dermal–epidermal boundary of glabrous skin in $\alpha_2\delta$-1$^{+/+}$ (***C***) and $\alpha_2\delta$-1$^{-/-}$ (***D***) mice. The dermal–epidermal junction is represented by the dotted line. Positive nerve profiles (stained with PGP 9.5 in red) crossing the dermal–epidermal junction are counted (arrows). Scale bar, 20 μm.

DRG neurons from $\alpha_2\delta$-1$^{+/+}$ and $\alpha_2\delta$-1$^{-/-}$ mice differ in their responsiveness to TRP channel agonists

Sensory neurons are broadly divided into mechanoreceptors, thermoreceptors, and nociceptors, and the differential expression of TRP channels is responsible for many of their distinctive somatosensory properties (Hjerling-Leffler et al., 2007). As shown in Figure 5*A*, we examined these properties by using Ca^{2+} imaging while exposing DRG neurons from $\alpha_2\delta$-1$^{+/+}$ and $\alpha_2\delta$-1$^{-/-}$ mice to sequential application of different TRP channel agonists. In the first set of experiments, MO (100 μM, 20 s) was applied to activate TRPA1, followed by menthol (ME, 500 μM, 30 s) to activate TRPM8, and finally capsaicin (CAPS or C, 1 μM, 10 s) to activate TRPV1. After the final agonist application, cells were stimulated with high potassium (K, 60 mM, 10 s) to assess cell viability. In a second set of experiments, another TRPA1 agonist CA was also applied. The agonist sequence in the second set was 250 μM ME for 30 s, followed by 100 μM CA for 60 s, followed by 1 μM CAPS for 5 s.

As shown in Figure 5*B*, the proportion of $\alpha_2\delta$-1$^{+/+}$ and $\alpha_2\delta$-1$^{-/-}$ cells responding to MO (applied in the first agonist sequence) was not significantly different. Furthermore, the proportion of $\alpha_2\delta$-1$^{+/+}$ cells and $\alpha_2\delta$-1$^{-/-}$ cells responding to 100 μM CA in the second agonist sequence was also not significantly different (49.6 ± 4.6% of $\alpha_2\delta$-1$^{+/+}$ cells; $n = 17$ coverslips), compared with 50.6 ± 3.4% of $\alpha_2\delta$-1$^{-/-}$ cells ($n = 19$ coverslips). In contrast, a significantly higher proportion of $\alpha_2\delta$-1$^{-/-}$ cells responded to CAPS (Fig. 5*B*; a 27% increase, data pooled from both agonist sequences). Furthermore, a significantly lower proportion of $\alpha_2\delta$-1$^{-/-}$ cells responded to ME (250 or 500 μM for 30 s) compared with $\alpha_2\delta$-1$^{+/+}$ cells (Fig. 5*B*; a 33% decrease, data pooled from both agonist sequences).

To determine whether the changes in proportion of cells responding to CAPS and ME reflected an altered sensitivity to agonist, or a change in the number of DRG neurons expressing these receptors, we next compared the amplitude of TRP channel agonist responses measured in $\alpha_2\delta$-1$^{+/+}$ and $\alpha_2\delta$-1$^{-/-}$ DRG neurons. As shown in Figure 5*C*, MO, CA, and CAPS all evoked a significantly higher fura-2 AM ratio peak in $\alpha_2\delta$-1$^{-/-}$ compared with $\alpha_2\delta$-1$^{+/+}$ cells. In contrast, there was no significant difference in the peak response between $\alpha_2\delta$-1$^{-/-}$ and $\alpha_2\delta$-1$^{+/+}$ cells evoked by either 250 μM ME (Fig. 5*C*) or 500 μM ME (ratio in $\alpha_2\delta$-1$^{+/+}$ cells: 2.28 ± 0.14, $n = 33$; ratio in $\alpha_2\delta$-1$^{-/-}$ cells: 2.51 ± 0.31, $n = 21$). There was also no significant difference in the peak response between $\alpha_2\delta$-1$^{-/-}$ and $\alpha_2\delta$-1$^{+/+}$ DRGs evoked by 30 s application of 20 μM WS-12, a menthol derivative (Bodding et al., 2007). The ratio was 2.21 ± 0.28 ($n = 9$) and 2.66 ± 0.13 ($n = 19$) in $\alpha_2\delta$-1$^{+/+}$ and $\alpha_2\delta$-1$^{-/-}$ cells, respectively ($p = 0.11$). This suggests that the loss of $\alpha_2\delta$-1 does not affect the function of TRPM8 channels and is not the reason for the smaller number of cells responding to ME. Furthermore, we found no significant change in TRPM8, TRPA1, or TRPV1 mRNA levels, in $\alpha_2\delta$-1$^{-/-}$ compared with $\alpha_2\delta$-1$^{+/+}$ DRGs (Fig. 6*A*), suggesting that compensatory changes in receptor expression are not responsible for the differences between $\alpha_2\delta$-1$^{+/+}$ and $\alpha_2\delta$-1$^{-/-}$ cells observed in the Ca^{2+} imaging experiments. In

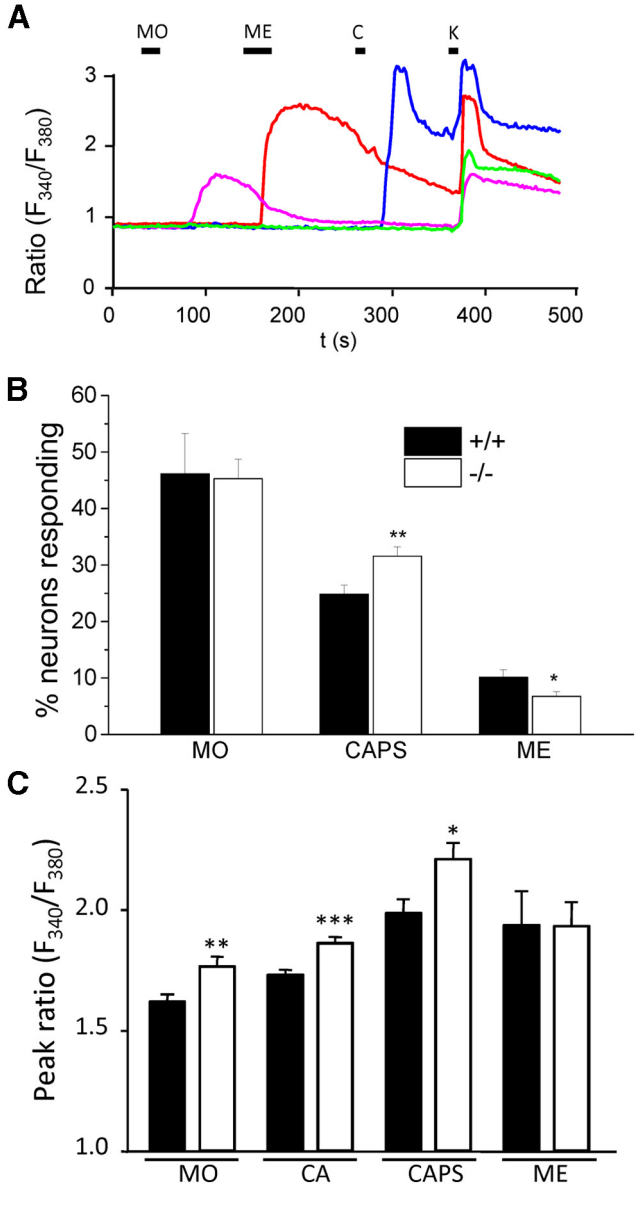

Figure 5. TRPA1, TRPV1, and TRPM8 responses in $\alpha_2\delta$-1$^{+/+}$ and $\alpha_2\delta$-1$^{-/-}$ DRG neurons. ***A***, Representative traces showing changes in cytoplasmic Ca^{2+} activity (fura-2 AM fluorescence ratio: ratio (F_{340}/F_{380})) in response to the TRPA1 agonist MO (100 μM, applied for 20 s), the TRPM8 agonist ME (500 μM, 30 s), the TRPV1 agonist CAPS (1 μM, 10 s), and 60 mM K^+ (K, 10 s) in $\alpha_2\delta$-1$^{+/+}$ neurons. ***B***, Quantification of percentage of $\alpha_2\delta$-1$^{+/+}$ (black bars) and $\alpha_2\delta$-1$^{-/-}$ (white bars) DRG neurons responding to MO (100 μM for 20 s, left), CAPS (1 μM for 5 or 10 s, middle), and ME (250 or 500 μM for 30 s, right). The number of responses to each agonist was normalized to number of responses to 60 mM K^+ per coverslip. Error bars indicate SEM. Statistical analysis was as follows: unpaired Student's *t* test comparing $\alpha_2\delta$-1$^{+/+}$ and $\alpha_2\delta$-1$^{-/-}$ responses: MO response, $p = 0.90$ ($n = 13$ $\alpha_2\delta$-1$^{+/+}$ and $n = 18$ $\alpha_2\delta$-1$^{-/-}$ coverslips); CAPS response, $p = 0.005$ ($n = 29$ $\alpha_2\delta$-1$^{+/+}$ and $n = 36$ $\alpha_2\delta$-1$^{-/-}$ coverslips); ME response, $p = 0.028$ ($n = 30$ $\alpha_2\delta$-1$^{+/+}$ and $n = 37$ $\alpha_2\delta$-1$^{-/-}$ coverslips). In total, $n = 982$ $\alpha_2\delta$-1$^{+/+}$ and $n = 1151$ $\alpha_2\delta$-1$^{-/-}$ cells were analyzed. ***C***, Peak fura-2 AM fluorescence ratio (peak ratio: (F_{340}/F_{380})) for MO, CA, CAPS, and ME responses. Error bars indicate SEM. Statistical analysis was as follows: unpaired Student's *t* test, comparing $\alpha_2\delta$-1$^{+/+}$ and $\alpha_2\delta$-1$^{-/-}$ neurons: MO peak response, $p < 0.003$ ($n = 290$ $\alpha_2\delta$-1$^{+/+}$, $n = 247$ $\alpha_2\delta$-1$^{-/-}$ neurons); CA peak response, $p = 0.0002$ ($n = 230$ $\alpha_2\delta$-1$^{+/+}$, $n = 325$ $\alpha_2\delta$-1$^{-/-}$ neurons); CAPS peak response, $p = 0.011$ ($n = 189$ $\alpha_2\delta$-1$^{+/+}$, $n = 191$ $\alpha_2\delta$-1$^{-/-}$ neurons); ME peak response (250 μM), $p = 0.98$ ($n = 55$ $\alpha_2\delta$-1$^{+/+}$, $n = 49$ $^{-/-}$ neurons). *$p < 0.05$. **$p < 0.01$. ***$p < 0.001$.

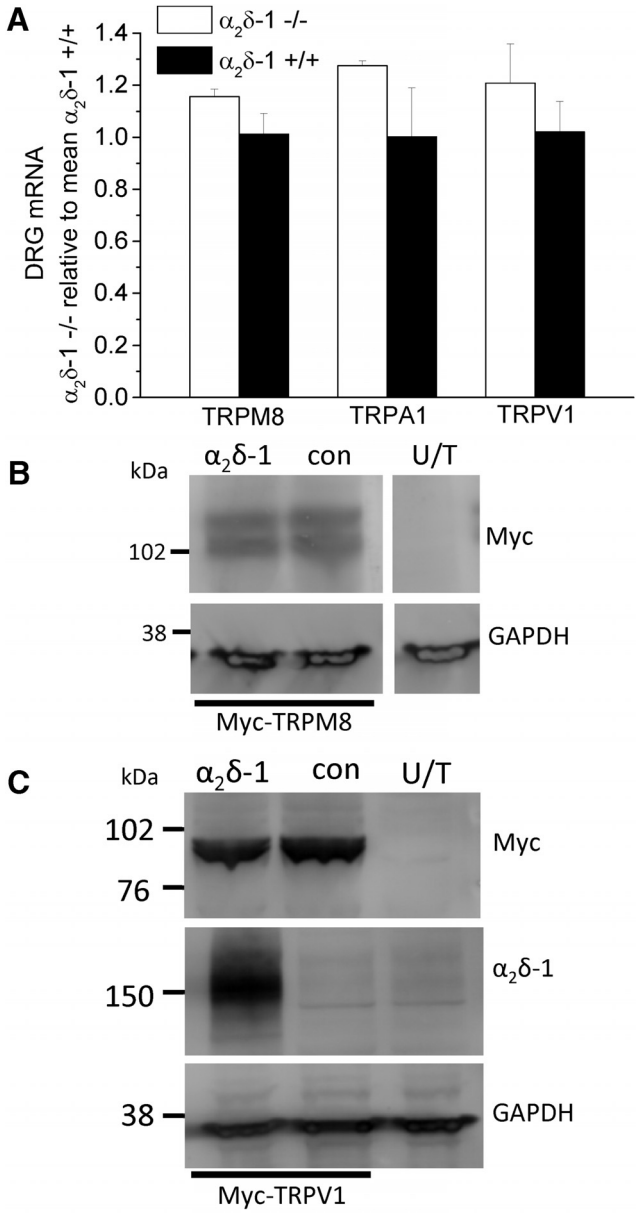

Figure 6. TRP channel mRNA and protein expression. ***A***, TRPM8, TRPA1, and TRPV1 mRNA levels in $\alpha_2\delta$-1$^{-/-}$ (white bar) and $\alpha_2\delta$-1$^{+/+}$ (black bar) DRGs ($n = 3$), normalized to the mean $\alpha_2\delta$-1$^{+/+}$ mRNA values. ***B***, ***C***, TRPM8 (***B***) and TRPV1 (***C***) expression, after transfection in tsA-201 cells, detected by their associated myc tag (top), was not affected by coexpression of $\alpha_2\delta$-1 (lane 1), compared with a control protein β1b (lane 2). No signal was observed in WCL from untransfected (U/T) tsA-201 cells (lane 3). Bottom, GAPDH loading controls. ***C***, $\alpha_2\delta$-1 expression is also shown (middle). All lanes are from the same gel. Data are representative of $n = 2$ experiments.

addition, there was no effect of $\alpha_2\delta$-1 coexpression on TRPM8 or TRPV1 expression levels when they were coexpressed in tsA-201 cells (Fig. 6*B*,*C*). Piezo2 has been shown to be involved in mechanosensation (Coste et al., 2012) and in mechanical allodynia (Eijkelkamp et al., 2013). However, we found that the Piezo2 mRNA levels were not altered in DRGs from $\alpha_2\delta$-1$^{-/-}$ mice, the level being 94.7 ± 7.8% in $\alpha_2\delta$-1$^{-/-}$ DRGs, relative to $\alpha_2\delta$-1 DRGs ($n = 3$; unpaired *t* test, $p = 0.62$).

Calcium channel currents are reduced in DRGs from $\alpha_2\delta$-1$^{-/-}$ compared with $\alpha_2\delta$-1$^{+/+}$ mice

Calcium channel currents were recorded using 2 mM Ba^{2+} as the charge carrier, from small and medium DRG neurons, cultured

from $\alpha_2\delta$-1$^{-/-}$ and $\alpha_2\delta$-1$^{+/+}$ mice (Fig. 7). Current density–voltage (I-V) relationships were measured 30 ms after the start of depolarization (Fig. 7*A*,*B*). The peak current density was 27% smaller at 0 mV and 30% smaller at 10 mV, in $\alpha_2\delta$-1$^{-/-}$ compared with $\alpha_2\delta$-1$^{+/+}$ DRG neurons, but there was no significant shift in the voltage dependence of activation of the currents. In experiments using ω-conotoxin GVIA (1 μM) to block N-type currents (Fig. 7*C*,*D*), this toxin inhibited the peak Ba^{2+} currents in $\alpha_2\delta$-1$^{+/+}$ DRGs by 51% at 0 mV, (54% at 10 mV), and that in $\alpha_2\delta$-1$^{-/-}$ DRGs by 55% at 0 mV (52% at 10 mV) (compare Fig. 7*A* with Fig. 7*C*), indicating that there is a similar component of N-type current in $\alpha_2\delta$-1$^{-/-}$ and $\alpha_2\delta$-1$^{+/+}$ DRG somata.

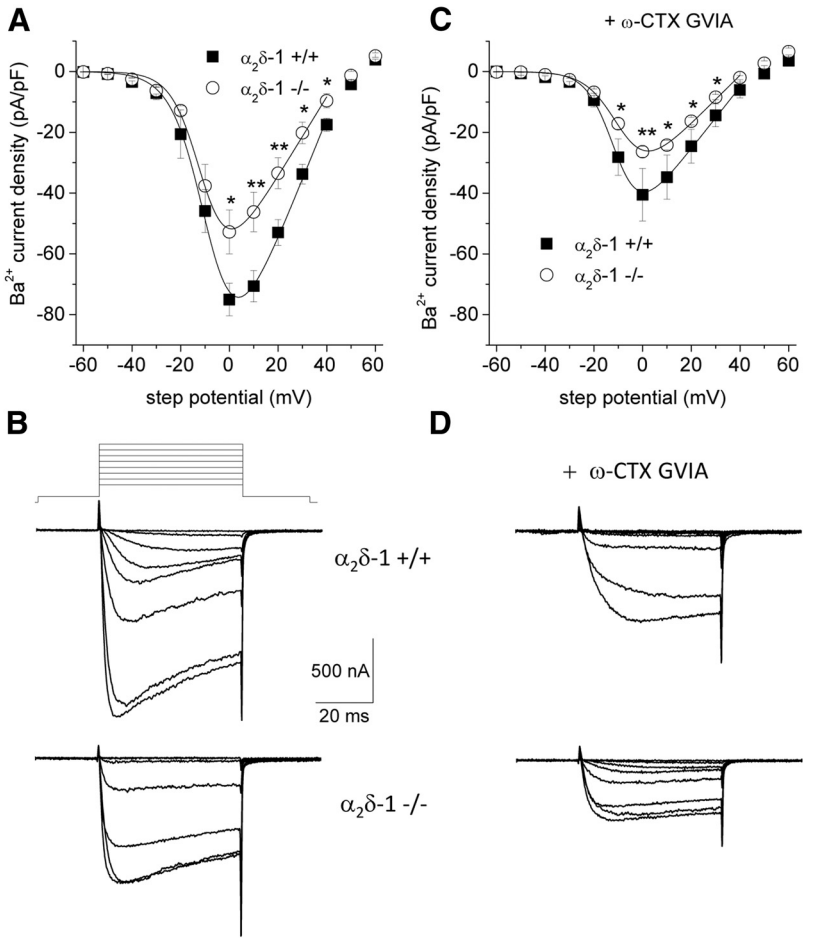

Figure 7. Calcium channel currents in $\alpha_2\delta$-1$^{+/+}$ and $\alpha_2\delta$-1$^{-/-}$ DRG neurons. ***A***, Calcium channel current density-voltage relationship for $\alpha_2\delta$-1$^{+/+}$ (closed squares, $n = 19$ cells, 4 mice) and $\alpha_2\delta$-1$^{-/-}$ (open circles, $n = 29$ cells, 5 mice) DRG neurons. Mean data were fit between −60 and 40 mV with a modified Boltzmann relationship (see Materials and Methods). For $\alpha_2\delta$-1$^{+/+}$, the $V_{50,act}$ was −10.2 mV and for $\alpha_2\delta$-1$^{-/-}$, the $V_{50,act}$ was −8.17 mV. ***B***, Representative current traces under the two conditions: $\alpha_2\delta$-1$^{+/+}$ (top) and $\alpha_2\delta$-1$^{-/-}$ (bottom). Top, Voltage protocol. Holding potential −90 mV, test potentials −60 to 10 mV in 10 mV steps. ***C***, Calcium channel current density-voltage relationship for $\alpha_2\delta$-1$^{+/+}$ (closed squares, $n = 7$ cells, 4 mice) and $\alpha_2\delta$-1$^{-/-}$ (open circles, $n = 25$ cells, 7 mice) for DRG neurons after preincubation for 15 min with ω-conotoxin GVIA (ω-CTX GVIA, 1 μM); otherwise as in ***A***. For $\alpha_2\delta$-1$^{+/+}$, the $V_{50,act}$ was −7.85 mV and for $\alpha_2\delta$-1$^{-/-}$, the $V_{50,act}$ was −10.3 mV. ***D***, Representative current traces under the two conditions, as in ***B***. Data were compared by two-way ANOVA, followed by the Tukey Honest Significant Differences test. ***A***, ***C***, The statistical significance of the difference in current density between $\alpha_2\delta$-1$^{+/+}$ and $\alpha_2\delta$-1$^{-/-}$ is indicated: *$p < 0.05$, **$p < 0.01$. There was no effect of ω-conotoxin GVIA on the difference in current density between the mouse genotypes.

$\alpha_2\delta$-1$^{-/-}$ mice develop delayed mechanical hypersensitivity after PSNL

We next sought to examine the development of mechanical and cold hypersensitivity in the absence of $\alpha_2\delta$-1, as the upregulation of this subunit has been shown to correlate with the development of neuropathic-like behaviors (Li et al., 2004). Baseline testing was performed 5 d before PSNL surgery and then repeated on postoperative days 3, 7, 9, 11, and 14. After surgery, mice groomed normally and maintained presurgery body weights. The $\alpha_2\delta$-1$^{+/+}$ mice developed rapid mechanical hypersensitivity on the injured side after PSNL, with significant increases in withdrawal frequency to the 0.4 g von Frey filament, compared with contralateral responses from day 3 onwards, and to $\alpha_2\delta$-1$^{+/+}$ sham responses from day 7 onwards (Fig. 8*A*). The ipsilateral withdrawal frequencies for $\alpha_2\delta$-1$^{-/-}$ mice were reduced compared with $\alpha_2\delta$-1$^{+/+}$ mice at days 3, 7, 9, and 11 and only differed from contralateral responses from day 11 onwards (Fig. 8*B*). The $\alpha_2\delta$-1$^{+/+}$ sham mice did not display any behavioral changes after surgery for the duration of the 2 week observation period (Fig. 8*C*).

Cold hypersensitivity after PSNL was not markedly altered in $\alpha_2\delta$-1$^{-/-}$ mice, and was an infrequent occurrence after surgery in both genotypes. The $\alpha_2\delta$-1$^{+/+}$ ipsilateral responses differed significantly from the contralateral responses on days 11 and 14 (Fig. 8*D*), $\alpha_2\delta$-1$^{-/-}$ ipsilateral responses differed significantly from the contralateral responses on days 3, 7, and 9 (Fig. 8*E*); however, no significant difference was observed between the $\alpha_2\delta$-1$^{+/+}$ and $\alpha_2\delta$-1$^{-/-}$ ipsilateral responses. The $\alpha_2\delta$-1$^{+/+}$ sham ipsilateral responses did not differ from the contralateral side (Fig. 8*F*).

Anti-hyperalgesic efficacy of pregabalin is lost in $\alpha_2\delta$-1$^{-/-}$ mice after PSNL

The ability of pregabalin to attenuate mechanical hypersensitivity was examined in $\alpha_2\delta$-1$^{+/+}$ and $\alpha_2\delta$-1$^{-/-}$ 14 d after PSNL. Mechanical hypersensitivity was tested before administration of either vehicle or 10 mg/kg pregabalin, and repeated 30, 60, and 90 min after dosing. In $\alpha_2\delta$-1$^{+/+}$ mice, pregabalin reduced withdrawal frequency on the injured ipsilateral side compared with predrug values at 30 min after dosing, and to the vehicle-treated group at 30 and 60 min after dosing. Contralateral responses were not altered by vehicle or pregabalin treatment (Fig. 8*G*). In $\alpha_2\delta$-1$^{-/-}$ mice, pregabalin did not affect mechanical hypersensitivity compared with predrug withdrawal frequencies or the vehicle-treated group. Contralateral responses were also unaffected by both treatments (Fig. 8*H*).

$\alpha_2\delta$-1 mRNA is upregulated after PSNL in $\alpha_2\delta$-1$^{+/+}$ DRGs, but other Ca_V auxiliary subunits do not compensate for $\alpha_2\delta$-1 in −/− DRGs

Nerve injury in animal models of chronic pain causes changes in the expression of a plethora of genes and their gene products (Costigan et al., 2002). These changes include the upregulation of $\alpha_2\delta$-1 (Newton et al., 2001). Using quantitative PCR

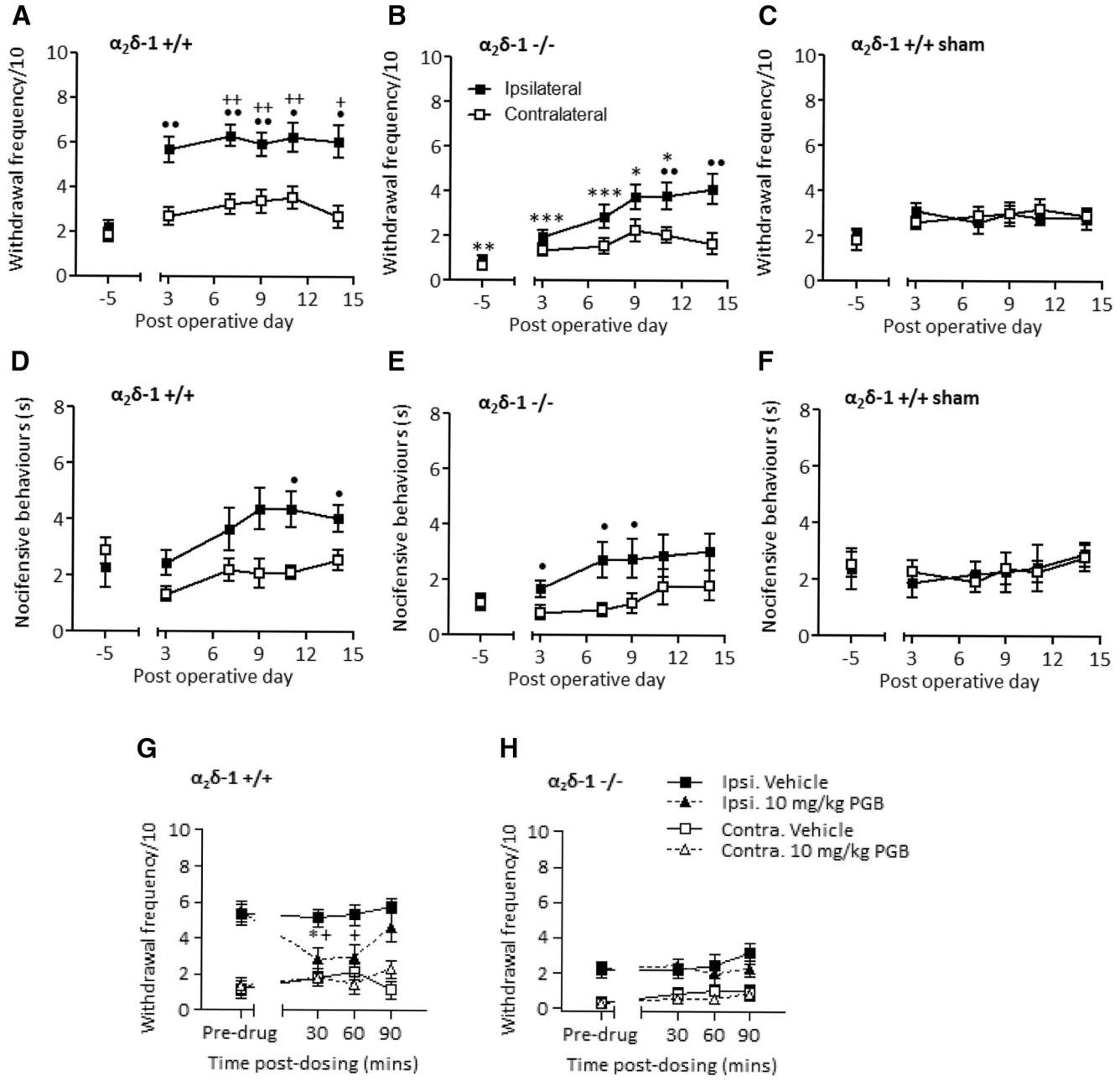

Figure 8. Development of mechanical and cold hypersensitivity after PSNL. The same legend applies for all data. ■ represents the ipsilateral side; and □ represents the contralateral side. ***A***, Increased frequency of ipsilateral withdrawals to mechanical stimulation (0.4 g von Frey) compared with contralateral for $\alpha_2\delta$-1$^{+/+}$ group. ***B***, Delayed increase in frequency of ipsilateral withdrawals to mechanical stimulation compared with contralateral for $\alpha_2\delta$-1$^{-/-}$ group. ***C***, Unaltered frequency of ipsilateral withdrawals to mechanical stimulation compared with contralateral for $\alpha_2\delta$-1$^{+/+}$ sham group (Kruskal-Wallis, paired comparisons made with Dunn's *post hoc* test and Bonferroni correction). *n* for +/+ = 16, *n* for −/− = 16, *n* for +/+ sham-operated = 10. ***D***, Increased duration of $\alpha_2\delta$-1$^{+/+}$ ipsilateral response to cooling stimulation compared with contralateral. ***E***, Increased duration of $\alpha_2\delta$-1$^{-/-}$ ipsilateral response to cooling stimulation compared with contralateral. ***F***, Unaltered duration of $\alpha_2\delta$-1$^{+/+}$ sham ipsilateral response to cooling stimulation compared with contralateral (two-way repeated-measures ANOVA, paired comparisons made with Bonferroni's *post hoc* test). *n* for +/+ = 11, *n* for −/− = 13, *n* for +/+ sham = 7. *Statistically significant differences between $\alpha_2\delta$-1$^{+/+}$ and $\alpha_2\delta$-1$^{-/-}$ mice. $^{+}$Statistically significant differences between $\alpha_2\delta$-1$^{+/+}$ and $\alpha_2\delta$-1$^{+/+}$ sham groups. ●Statistically significant differences between ipsilateral and contralateral. ***G***, The 10 mg/kg pregabalin attenuates mechanical hypersensitivity in $\alpha_2\delta$-1$^{+/+}$ mice (symbols given in key above ***H***; Friedman test $p < 0.01$, paired comparisons made with Wilcoxon test). $n = 6$ for all groups. *Statistically significant difference of response in pregabalin-treated mice, compared with predrug withdrawal frequency. $^{+}$Statistically significant differences between ipsilateral vehicle-treated and ipsilateral pregabalin-treated responses. *$p < 0.05$. **$p < 0.01$. ***$p < 0.001$. Data represent mean ± SEM. PGB, Pregabalin; Ipsi., ipsilateral; Contra., contralateral. ***H***, Efficacy of pregabalin is lost in $\alpha_2\delta$-1$^{-/-}$ mice. *n* for vehicle = 6, *n* for pregabalin-treated = 7.

14 d after PSNL, we found that the $\alpha_2\delta$-1 mRNA level was significantly increased by >100% in ipsilateral L3-L5 DRGs from $\alpha_2\delta$-1$^{+/+}$ mice compared with sham-operated $\alpha_2\delta$-1$^{+/+}$ mice (Fig. 9*A*). We next investigated the expression of the other two $\alpha_2\delta$ isoforms present in DRGs (i.e., $\alpha_2\delta$-2 and $\alpha_2\delta$-3). We found that their expression level did not change in $\alpha_2\delta$-1$^{+/+}$ mice after PSNL compared with $\alpha_2\delta$-1$^{+/+}$ mice after sham surgery (Fig. 9*B*,*C*, black bars). Moreover, the expression levels of $\alpha_2\delta$-2 and $\alpha_2\delta$-3 mRNA in $\alpha_2\delta$-1$^{-/-}$ PSNL mice were not significantly different from the levels found in $\alpha_2\delta$-1$^{+/+}$ sham and PSNL mice (Figs. 9*B*,*C*, white bar compared with black PSNL bar). This indicates that neither of the

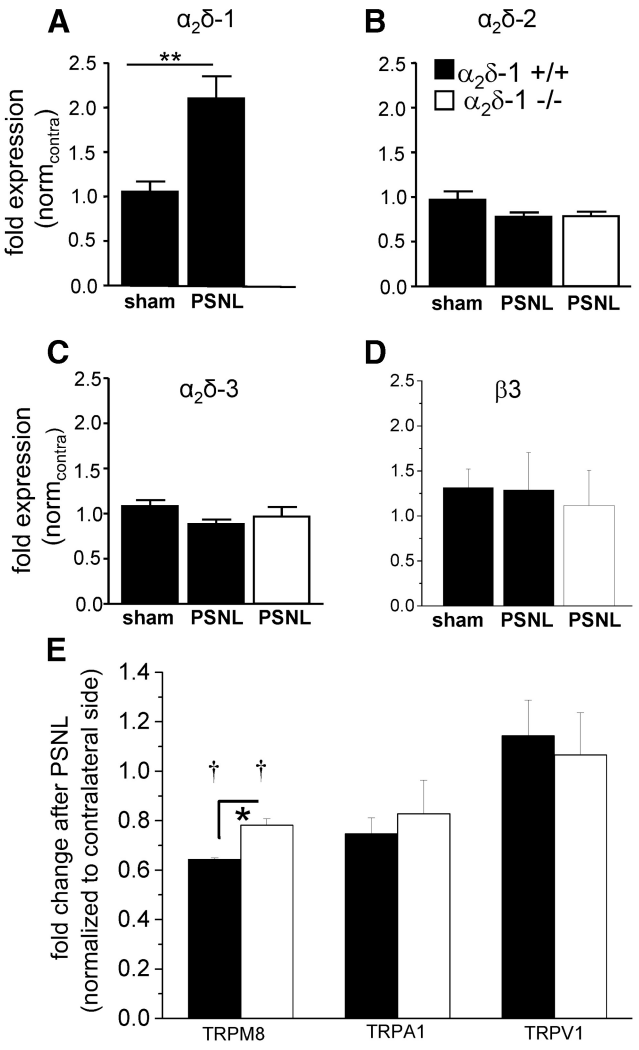

Figure 9. PSNL-mediated ipsilateral changes of mRNA of neuropathy markers in $\alpha_2\delta$-1$^{+/+}$ and $\alpha_2\delta$-1$^{-/-}$ DRGs. The legend applies to all parts of the figure. ***A***, Q-PCR results for $\alpha_2\delta$-1 mRNA levels (fold expression (norm$_{contra}$)) in pooled L3-L5 ipsilateral DRGs from sham-operated ($n = 9$) or PSNL-operated ($n = 7$) $\alpha_2\delta$-1$^{+/+}$ mice (black bars), 14 d after surgery. Data are normalized to the respective contralateral side. Error bars indicate SEM. Statistical analysis was performed using one-way ANOVA with $p = 0.003$ using Bonferroni's post test. No data are included for the $\alpha_2\delta$-1$^{-/-}$ DRGs because of the gene disruption. ***B***, Q-PCR results for $\alpha_2\delta$-2 mRNA levels (fold expression (norm$_{contra}$)) in pooled L3-L5 ipsilateral DRGs from sham-operated ($n = 9$) or PSNL-operated ($n = 7$) $\alpha_2\delta$-1$^{+/+}$ mice (black bars) or PSNL-operated $\alpha_2\delta$-1$^{-/-}$ mice (white bar, $n = 7$), 14 d after surgery. Data are normalized to the respective contralateral side. Error bars indicate SEM. Statistical analysis: one-way ANOVA with $p = 0.11$. ***C***, Q-PCR results for $\alpha_2\delta$-3 mRNA levels (fold expression (norm$_{contra}$)) in pooled L3-L5 ipsilateral DRGs from sham-operated ($n = 9$) or PSNL-operated ($n = 7$) $\alpha_2\delta$-1$^{+/+}$ mice (black bars) or PSNL-operated $\alpha_2\delta$-1$^{-/-}$ mice (white bar, $n = 7$), 14 d after surgery. Data are normalized to the respective contralateral side. Error bars indicate SEM. Statistical analysis: one-way ANOVA with $p = 0.21$. ***D***, Q-PCR results for β3 mRNA levels (fold expression (norm$_{contra}$)) in pooled L3-L5 ipsilateral DRGs from sham-operated ($n = 9$) or PSNL-operated ($n = 7$) $\alpha_2\delta$-1$^{+/+}$ mice (black bars) or PSNL-operated $\alpha_2\delta$-1$^{-/-}$ mice (white bar, $n = 6$), 14 d after surgery. Data are normalized to the respective contralateral side. Error bars indicate SEM. Statistical analysis: one-way ANOVA with Bonferroni's multiple-comparison test, $p > 0.05$ for all comparisons. ***E***, Q-PCR results for TRPM8, TRPA1, and TRPV1 mRNA levels (fold expression) in pooled L3-L5 ipsilateral DRGs from PSNL-operated $\alpha_2\delta$-1$^{+/+}$ mice (black bars $n = 3$) or PSNL-operated $\alpha_2\delta$-1$^{-/-}$ mice (white bars, $n = 3$), 14 d after surgery. Data are normalized to the respective contralateral side. Error bars indicate SEM. Statistical analysis shows that TRPM8 mRNA ratios for $\alpha_2\delta$-1$^{+/+}$ and $\alpha_2\delta$-1$^{-/-}$ DRGs are significantly less than a theoretical value of 1: †$p = 0.0003$ and $p = 0.0142$, respectively (one-sample t test). The difference between $\alpha_2\delta$-1$^{+/+}$ and $\alpha_2\delta$-1$^{-/-}$ TRPM8 ratios is also statistically significant: *$p = 0.068$ (Student's t test).

other two $\alpha_2\delta$ isoforms compensates for the absence of $\alpha_2\delta$-1 upregulation after PSNL in $\alpha_2\delta$-1$^{-/-}$ mice.

Ca$_V\beta$3, which is the main β subunit in DRGs, and has been found in one study to be upregulated in rat DRGs after SNL (Li et al., 2012); however, here we found the β3 mRNA level was not altered in DRGs by PSNL, either in $\alpha_2\delta$-1$^{+/+}$ or $\alpha_2\delta$-1$^{-/-}$ mice (Fig. 9*D*).

Investigation of TRP channel mRNA levels in $\alpha_2\delta$-1$^{+/+}$ and $\alpha_2\delta$-1$^{-/-}$ DRGs after PSNL

We compared mRNA levels for TRPM8, TRPA1, and TRPV1 in $\alpha_2\delta$-1$^{+/+}$ and $\alpha_2\delta$-1$^{-/-}$ DRGs, normalizing the data on the ipsilateral side after PSNL to that on the corresponding contralateral side. We found that TRPM8 mRNA was significantly reduced ipsilateral to PSNL compared with the level in the corresponding contralateral DRGs, as previously observed for another nerve injury model (Caspani et al., 2009), but there was a smaller reduction in the $\alpha_2\delta$-1$^{-/-}$ than in $\alpha_2\delta$-1$^{+/+}$ DRGs (Fig. 9*E*).

ATF3 mRNA and NPY protein are upregulated normally after PSNL in $\alpha_2\delta$-1$^{-/-}$ DRGs

We next compared the mRNA levels of ATF3, a neuronal marker for nerve injury (Tsujino et al., 2000), in $\alpha_2\delta$-1$^{+/+}$ and $\alpha_2\delta$-1$^{-/-}$ DRGs. We found that, 14 d after PSNL, ATF3 mRNA was significantly upregulated in both $\alpha_2\delta$-1$^{+/+}$ and $\alpha_2\delta$-1$^{-/-}$ DRGs compared with DRGs taken from $\alpha_2\delta$-1$^{+/+}$ sham-operated mice (Fig. 10*A*). Moreover, the upregulation of ATF3 in $\alpha_2\delta$-1$^{-/-}$ DRGs was not significantly different from the upregulation in $\alpha_2\delta$-1$^{+/+}$ tissue.

Immunofluorescence staining in DRGs 14 d after PSNL confirmed the ipsilateral upregulation of $\alpha_2\delta$-1 (green) in $\alpha_2\delta$-1$^{+/+}$ L4 DRGs compared with the contralateral side (Fig. 10*B*, upper row, first and third panels). There was no detectable $\alpha_2\delta$-1 staining in sections of ipsilateral or contralateral L4 DRGs from $\alpha_2\delta$-1$^{-/-}$ mice (Fig. 10*B*, upper row, second and fourth panels). Staining for neuropeptide Y (NPY, red), another marker for nerve injury (Wakisaka et al., 1992; Ruscheweyh et al., 2007) in the same sections, showed that NPY was upregulated in the ipsilateral DRGs from both $\alpha_2\delta$-1$^{+/+}$ and $\alpha_2\delta$-1$^{-/-}$ mice (Fig. 10*B*, lower row, first and second panels), whereas the staining was virtually absent from the contralateral side (Fig. 10*B*, lower row, third and fourth panels). We then quantified the NPY staining by counting the number of NPY-positive cells per section (Fig. 10*C*). There was no significant difference in the number of NPY-positive cells in ipsilateral and contralateral sections from L3-L5 DRGs from $\alpha_2\delta$-1$^{+/+}$ compared with $\alpha_2\delta$-1$^{-/-}$ mice 14 d after PSNL. The quantification also showed that PSNL mainly affected the L3 and L4 DRG neurons and axons.

Discussion

This study examined whether $\alpha_2\delta$-1 is involved in baseline somatosensory functions and in development of neuropathic pain. We found that $\alpha_2\delta$-1 knock-out mice show markedly reduced behavioral sensitivity to mechanical and cold stimuli, with no change in withdrawal threshold for noxious heat. $\alpha_2\delta$-1 is expressed in most excitable tissues, including peripheral and central neurons (Cole et al., 2005; Taylor and Garrido, 2008). In this global $\alpha_2\delta$-1 knock-out model, altered behavioral sensitivity could therefore be attributed to differences in supraspinal circuits as well as spinal and somatosensory neurons. Our data strongly support a peripheral and spinal role for $\alpha_2\delta$-1 in modulating sensitivity to these stimuli. The behavioral profile was, in part, reflected by attenuated mechanical responses of dorsal horn neu-

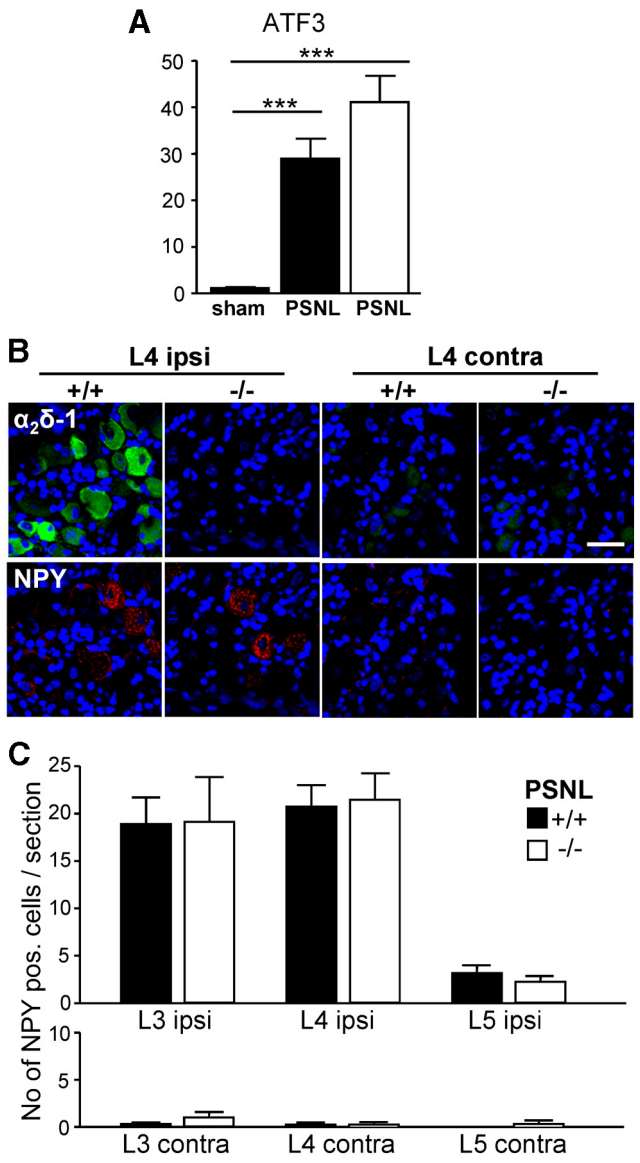

Figure 10. PSNL-mediated ipsilateral changes of mRNA and protein levels of neuropathy markers in $\alpha_2\delta$-1$^{+/+}$ and $\alpha_2\delta$-1$^{-/-}$ DRGs. ***A***, Q-PCR results for ATF3 mRNA levels (fold expression) in pooled L3-L5 ipsilateral DRGs from sham-operated ($n = 9$) or PSNL-operated ($n = 7$) $\alpha_2\delta$-1$^{+/+}$ mice (black bars) or PSNL-operated $\alpha_2\delta$-1$^{-/-}$ mice (white bar, $n = 7$) 14 d after surgery. Data are normalized to the respective contralateral side. ***$p < 0.001$ (one-way ANOVA and Bonferroni's *post hoc* test). ATF3 mRNA levels in PSNL-operated $\alpha_2\delta$-1$^{+/+}$ were not significantly different from PSNL-operated $\alpha_2\delta$-1$^{-/-}$ mice. ***B***, Representative immunofluorescence images of ipsilateral (ipsi) and contralateral (contra) L4 DRG sections from $\alpha_2\delta$-1$^{+/+}$ and $\alpha_2\delta$-1$^{-/-}$ mice after PSNL. Double immunofluorescence staining for $\alpha_2\delta$-1 (green) and NPY (red); blue represents nuclear staining. Scale bar, 100 μm. ***C***, Quantification of NPY-positive cells per section (number of NPY-positive cells/section) in ipsilateral and contralateral $\alpha_2\delta$-1$^{+/+}$ (black bars) and $\alpha_2\delta$-1$^{-/-}$ (white bars) L3-L5 DRGs 14 d after PSNL. Error bars indicate SEM. Statistical analysis was as follows: unpaired Student's *t* test comparing number of NPY-positive cells. $\alpha_2\delta$-1$^{+/+}$ and $\alpha_2\delta$-1$^{-/-}$ DRG sections: ipsilateral L3, $p = 0.97$ ($n = 18$ $\alpha_2\delta$-1$^{+/+}$ sections, $n = 19$ $\alpha_2\delta$-1$^{-/-}$ sections); ipsilateral L4, $p = 0.84$ ($n = 22$ $\alpha_2\delta$-1$^{+/+}$ sections, $n = 20$ $\alpha_2\delta$-1$^{-/-}$ sections); ipsilateral L5, $p = 0.37$ ($n = 13$ $\alpha_2\delta$-1$^{+/+}$ sections, $n = 13$ $\alpha_2\delta$-1$^{-/-}$ sections); contra L3, $p = 0.27$ ($n = 11$ $\alpha_2\delta$-1$^{+/+}$ sections, $n = 13$ $\alpha_2\delta$-1$^{-/-}$ sections); contra L4 contra, $p = 0.94$ ($n = 13$ $\alpha_2\delta$-1$^{+/+}$ sections, $n = 12$ $\alpha_2\delta$-1$^{-/-}$ sections); and contra L5, $p = 0.39$ ($n = 8$ $\alpha_2\delta$-1$^{+/+}$ sections, $n = 10$ $\alpha_2\delta$-1$^{-/-}$ sections).

rons, whereas thermal responses were unaffected. The lower presynaptic "input" after electrical stimulation in $\alpha_2\delta$-1$^{-/-}$ mice likely represents a decrease of synaptic transmitter release from primary afferents projecting to dorsal horn neurons, and the lack of change in windup also supports presynaptic alterations. However, there was no global reduction in primary afferent transmission via A and C-fibers, in terms of evoked responses and thresholds, suggesting no major changes in conduction of afferent nerves.

In addition to its association with calcium channels, $\alpha_2\delta$-1 has also been shown to mediate excitatory synaptogenesis via interaction with thrombospondin (Eroglu et al., 2009). At the spinal level, $\alpha_2\delta$-1 is strongly expressed in presynaptic terminals of primary afferents terminating in the superficial laminae (Bauer et al., 2009), whereas lamina V/VI dorsal horn neurons receive both direct and indirect input from Aβ, Aδ, and C fibers. The present study does not directly address whether there are differences between $\alpha_2\delta$-1$^{+/+}$ and $\alpha_2\delta$-1$^{-/-}$ mice in primary afferent synapse numbers. This hypothesis is certainly feasible and will be examined in the future, although the modality-specific deficits argue against global synaptic dysregulation in the dorsal horn.

It is of interest that the phenotype shown by $\alpha_2\delta$-1$^{-/-}$ mice (reduced mechanical and cold sensitivity, with no change in sensitivity to noxious heat) shows similarities with that observed in $Na_V1.8$ knock-out mice (Abrahamsen et al., 2008), and when $Na_V1.7$ is deleted selectively in $Na_V1.8$-positive nociceptors (Minett et al., 2012). TRPM8 is the principal detector of cool temperatures in mouse (Bautista et al., 2007; Colburn et al., 2007; Dhaka et al., 2007; Knowlton et al., 2013). Although these neurons constitute a minor proportion of all primary afferents, synaptic transmission in this population may be particularly dependent on $\alpha_2\delta$-1.

To examine the basis for the observed modality-specific differences in response between the $\alpha_2\delta$-1$^{+/+}$ and $\alpha_2\delta$-1$^{-/-}$ mice, we examined the properties of the DRG neurons. Although gross differences were absent, when examining responses to TRP agonists, we found that the proportion of cultured DRG neurons responding to ME was significantly reduced in $\alpha_2\delta$-1$^{-/-}$ mice, agreeing with the marked reduction in behavioral response to acetone cooling in naive $\alpha_2\delta$-1$^{-/-}$ mice. Nevertheless, our experiments do not provide evidence that his effect was the result of a reduction in TRPM8 mRNA. Mechanoreceptors have recently been shown to be made up of Piezo proteins (Coste et al., 2012); however, the reduced baseline response to mechanical stimuli in $\alpha_2\delta$-1$^{-/-}$ mice was not a result of reduced Piezo2 mRNA.

The sensor for noxious heat, TRPV1, is selectively expressed in small-medium DRG neurons (Kobayashi et al., 2005), which also express $\alpha_2\delta$-1 most strongly (Newton et al., 2001; Bauer et al., 2009). Surprisingly, we found an increase in the proportion of DRG neurons in $\alpha_2\delta$-1$^{-/-}$ mice responding to activation of TRPV1 receptors by CAPS *in vitro* and a small increase in the peak Ca^{2+} response to CAPS. This difference is in contrast to the lack of change in behavioral threshold for elevated temperatures, and the lack of significant difference in AP response of WDR neurons to thermal stimulation. We hypothesize that this might represent a compensatory upregulation at the cellular level of TRPV1 receptor function in $\alpha_2\delta$-1$^{-/-}$ DRG neurons, to counteract the reduction in primary afferent transmission resulting from the loss of $\alpha_2\delta$-1 at central terminals. However, we found no change in TRPV1 mRNA level in $\alpha_2\delta$-1$^{-/-}$ DRGs, suggesting that there is no difference at the level of transcription, indicating that the basis for the increased response to CAPS *in vitro* may have a translational or post-translational basis. Interestingly, TRPV1 protein has been found to be upregulated in uninjured sensory neurons, after partial nerve injury (Kim et al., 2008).

An alternative hypothesis to explain the reduction in baseline response to cooling and mechanical stimulation is that $\alpha_2\delta$-1 is

involved directly in the function of TRPM8 receptors and mechanoreceptors. Whether $\alpha_2\delta$-1, which is transported to peripheral as well as central terminals of DRG neurons (Bauer et al., 2009), is associated directly with any of the channels involved in peripheral mechanosensation or cold sensation will be the subject of future experiments.

We found, as expected, that $\alpha_2\delta$-1$^{-/-}$ DRG neurons exhibit significantly smaller calcium channel currents, but the proportion of N-type currents in the somata was similar between the genotypes, being 52–55%. DRG neurons have been found to contain a high proportion of N-type currents (50–70%) (Regan et al., 1991; Bell et al., 2004), together with L-type (Scroggs and Fox, 1991), T-type (in some subclasses,Carbone and Lux, 1984; Scroggs and Fox, 1992; Bell et al., 2004), and a small amount of P-type (Saegusa et al., 2001).

We also found a reduced level of $Ca_V2.2$ protein in brain and spinal cord synaptosomes, in agreement with the hypothesis that $\alpha_2\delta$-1 is important for trafficking Ca_V2 channels to presynaptic terminals (Hoppa et al., 2012). We have recently found that $\alpha_2\delta$ subunits play a key role in shaping DRG neuronal action potentials, with overexpression of $\alpha_2\delta$-1 shortening action potential duration (Hoppa et al., 2012). The mechanism may involve the known ability of $\alpha_2\delta$-1 to influence calcium current kinetics (Felix et al., 1997; Cantí et al., 2003; Tuluc et al., 2007) or the coupling of calcium channels to particular K^+ channels associated with action potential repolarization (Hoppa et al., 2012). DRG neurons show a spectrum of action potential duration, C-nociceptors showing the longest and Aα/β fibers the shortest duration. Action potential duration is inversely correlated with maximal firing frequency (Lawson, 2002). Thus upregulation of $\alpha_2\delta$-1 after nerve injury may allow DRGs to support an increased spontaneous action potential firing frequency and increased transmitter release in a DRG subtype-selective manner, an adaptive response that would be absent from $\alpha_2\delta$-1$^{-/-}$ mice.

After chronic sensory nerve injury, the $\alpha_2\delta$-1$^{-/-}$ mice show a marked delay in the development of mechanical hypersensitivity in the affected limb, with a significant difference between the ipsilateral and contralateral side only being observed at 11 d after PSNL, whereas for WT mice this difference was evident at the first time point measured (3 d). This implicates $\alpha_2\delta$-1 in the early establishment of chronic pain, but that other factors must also be involved in the development of central neuroplasticity leading to a long-term neuropathic state. Together with the deficit in baseline mechanical responses in naive $\alpha_2\delta$-1$^{-/-}$ mice, this suggests that synaptic transmission between the mechanosensitive DRG neurons and dorsal horn neurons is particularly sensitive to the loss of $\alpha_2\delta$-1 from primary afferent terminals.

We previously identified two mechanisms whereby $\alpha_2\delta$ subunits increase synaptic transmission (Hoppa et al., 2012). In hippocampal neurons, $\alpha_2\delta$ subunits increased the trafficking of $Ca_V2.1$ from cell body to synaptic boutons, although it was not determined whether more channels were inserted into the plasma membrane, as occurs in expression systems (Hendrich et al., 2008). Second, $\alpha_2\delta$ subunits increased synaptic vesicle release probability after an action potential, interpreted as increasing the proximity of channels to active zone release sites, involving local channel organization into slots associated with vesicular release (Hoppa et al., 2012).

There is an increasing body of evidence that the elevation of the $\alpha_2\delta$-1 subunit after nerve injury is key to the mechanism of action of the gabapentinoid drugs in neuropathic pain (Field et al., 2006; Dolphin, 2012). It is therefore likely that these drugs act on multiple $\alpha_2\delta$-mediated trafficking processes (Hendrich et al., 2008; Tran-Van-Minh and Dolphin, 2010), which have different time courses *in vivo*, an effect on $\alpha_2\delta$-1-associated channel trafficking from DRG somata to presynaptic terminal (Bauer et al., 2009), being a slower process than modification of channel localization/recycling at the active zone.

Another action of gabapentin is to inhibit synaptogenesis via interference with $\alpha_2\delta$-1–thrombospondin interactions (Eroglu et al., 2009), although it is unclear how this mechanism would participate in the observed rapid reduction in mechanical hypersensitivity. In addition, there are other permissive processes for the actions of gabapentinoids (Fehrenbacher et al., 2003; Suzuki et al., 2005; Doyon et al., 2013). Although gabapentinoids display similar affinity for $\alpha_2\delta$-1 and $\alpha_2\delta$-2 (Gong et al., 2001; Marais et al., 2001), pregabalin had no effect on mechanically evoked responses in $\alpha_2\delta$-1$^{-/-}$ mice, confirming that $\alpha_2\delta$-1 is the molecular target for the anti-hyperalgesic actions of pregabalin (Field et al., 2006). The $\alpha_2\delta$-1$^{-/-}$ mice now provide another tool to study the mechanism(s) of action of gabapentinoids.

References

Abrahamsen B, Zhao J, Asante CO, Cendan CM, Marsh S, Martinez-Barbera JP, Nassar MA, Dickenson AH, Wood JN (2008) The cell and molecular basis of mechanical, cold, and inflammatory pain. Science 321:702–705. CrossRef Medline

Barclay J, Balaguero N, Mione M, Ackerman SL, Letts VA, Brodbeck J, Cantí C, Meir A, Page KM, Kusumi K, Perez-Reyes E, Lander ES, Frankel WN, Gardiner RM, Dolphin AC, Rees M (2001) Ducky mouse phenotype of epilepsy and ataxia is associated with mutations in the *Cacna2d2* gene and decreased calcium channel current in cerebellar Purkinje cells. J Neurosci 21:6095–6104. Medline

Bauer CS, Nieto-Rostro M, Rahman W, Tran-Van-Minh A, Ferron L, Douglas L, Kadurin I, Sri Ranjan Y, Fernandez-Alacid L, Millar NS, Dickenson AH, Lujan R, Dolphin AC (2009) The increased trafficking of the calcium channel subunit $\alpha2\delta$-1 to presynaptic terminals in neuropathic pain is inhibited by the $\alpha2\delta$ ligand pregabalin. J Neurosci 29:4076–4088. CrossRef Medline

Bautista DM, Siemens J, Glazer JM, Tsuruda PR, Basbaum AI, Stucky CL, Jordt SE, Julius D (2007) The menthol receptor TRPM8 is the principal detector of environmental cold. Nature 448:204–208. CrossRef Medline

Bell TJ, Thaler C, Castiglioni AJ, Helton TD, Lipscombe D (2004) Cell-specific alternative splicing increases calcium channel current density in the pain pathway. Neuron 41:127–138. CrossRef Medline

Bödding M, Wissenbach U, Flockerzi V (2007) Characterisation of TRPM8 as a pharmacophore receptor. Cell Calcium 42:618–628. CrossRef Medline

Cantí C, Davies A, Dolphin AC (2003) Calcium channel $\alpha2\delta$ subunits: structure, function and target site for drugs. Curr Neuropharmacol 1:209–217. CrossRef

Cantí C, Nieto-Rostro M, Foucault I, Heblich F, Wratten J, Richards MW, Hendrich J, Douglas L, Page KM, Davies A, Dolphin AC (2005) The metal-ion-dependent adhesion site in the Von Willebrand factor-A domain of $\alpha2\delta$ subunits is key to trafficking voltage-gated Ca^{2+} channels. Proc Natl Acad Sci U S A 102:11230–11235. CrossRef Medline

Carbone E, Lux HD (1984) A low voltage-activated fully inactivating Ca channel in vertebrate sensory neurones. Nature 310:501–502. CrossRef Medline

Caspani O, Zurborg S, Labuz D, Heppenstall PA (2009) The contribution of TRPM8 and TRPA1 channels to cold allodynia and neuropathic pain. PLoS One 4:e7383. CrossRef Medline

Colburn RW, Lubin ML, Stone DJ Jr, Wang Y, Lawrence D, D'Andrea MR, Brandt MR, Liu Y, Flores CM, Qin N (2007) Attenuated cold sensitivity in TRPM8 null mice. Neuron 54:379–386. CrossRef Medline

Cole RL, Lechner SM, Williams ME, Prodanovich P, Bleicher L, Varney MA, Gu G (2005) Differential distribution of voltage-gated calcium channel $\alpha2\delta$ subunit mRNA-containing cells in the rat central nervous system and the dorsal root ganglia. J Comp Neurol 491:246–269. CrossRef Medline

Coste B, Xiao B, Santos JS, Syeda R, Grandl J, Spencer KS, Kim SE, Schmidt M, Mathur J, Dubin AE, Montal M, Patapoutian A (2012) Piezo proteins are pore-forming subunits of mechanically activated channels. Nature 483:176–181. CrossRef Medline

Costigan M, Befort K, Karchewski L, Griffin RS, D'Urso D, Allchorne A, Sitarski J, Mannion JW, Pratt RE, Woolf CJ (2002) Replicate high-density rat genome oligonucleotide microarrays reveal hundreds of regulated genes in the dorsal root ganglion after peripheral nerve injury. BMC Neurosci 3:16. CrossRef Medline

Costigan M, Scholz J, Woolf CJ (2009) Neuropathic pain: a maladaptive response of the nervous system to damage. Annu Rev Neurosci 32:1–32. CrossRef Medline

Dhaka A, Murray AN, Mathur J, Earley TJ, Petrus MJ, Patapoutian A (2007) TRPM8 is required for cold sensation in mice. Neuron 54:371–378. CrossRef Medline

Dickenson AH, Sullivan AF (1987) Evidence for a role of the NMDA receptor in the frequency dependent potentiation of deep rat dorsal horn nociceptive neurones following C fibre stimulation. Neuropharmacology 26:1235–1238. CrossRef Medline

Dolphin AC (2012) Calcium channel auxiliary $\alpha(2)\delta$ and β subunits: trafficking and one step beyond. Nat Rev Neurosci 13:542–555. CrossRef Medline

Doyon N, Ferrini F, Gagnon M, De Koninck Y (2013) Treating pathological pain: is KCC2 the key to the gate? Expert Rev Neurother 13:469–471. CrossRef Medline

Eijkelkamp N, Linley JE, Torres JM, Bee L, Dickenson AH, Gringhuis M, Minett MS, Hong GS, Lee E, Oh U, Ishikawa Y, Zwartkuis FJ, Cox JJ, Wood JN (2013) A role for Piezo2 in EPAC1-dependent mechanical allodynia. Nat Commun 4:1682. CrossRef Medline

Eroglu C, Allen NJ, Susman MW, O'Rourke NA, Park CY, Ozkan E, Chakraborty C, Mulinyawe SB, Annis DS, Huberman AD, Green EM, Lawler J, Dolmetsch R, Garcia KC, Smith SJ, Luo ZD, Rosenthal A, Mosher DF, Barres BA (2009) Gabapentin receptor $\alpha2\delta$-1 is a neuronal thrombospondin receptor responsible for excitatory CNS synaptogenesis. Cell 139:380–392. CrossRef Medline

Fehrenbacher JC, Taylor CP, Vasko MR (2003) Pregabalin and gabapentin reduce release of substance P and CGRP from rat spinal tissues only after inflammation or activation of protein kinase C. Pain 105:133–141. CrossRef Medline

Felix R, Gurnett CA, De Waard M, Campbell KP (1997) Dissection of functional domains of the voltage-dependent Ca^{2+} channel $\alpha2\delta$ subunit. J Neurosci 17:6884–6891. Medline

Ferron L, Davies A, Page KM, Cox DJ, Leroy J, Waithe D, Butcher AJ, Sellataray P, Bolsover S, Pratt WS, Moss FJ, Dolphin AC (2008) The stargazin-related protein gamma 7 interacts with the mRNA-binding protein heterogeneous nuclear ribonucleoprotein A2 and regulates the stability of specific mRNAs, including CaV2.2. J Neurosci 28:10604–10617. CrossRef Medline

Field MJ, Cox PJ, Stott E, Melrose H, Offord J, Su TZ, Bramwell S, Corradini L, England S, Winks J, Kinloch RA, Hendrich J, Dolphin AC, Webb T, Williams D (2006) Identification of the $\alpha2\delta$-1 subunit of voltage-dependent calcium channels as a novel molecular target for pain mediating the analgesic actions of pregabalin. Proc Natl Acad Sci U S A 103: 17537–17542. CrossRef Medline

Fuller-Bicer GA, Varadi G, Koch SE, Ishii M, Bodi I, Kadeer N, Muth JN, Mikala G, Petrashevskaya NN, Jordan MA, Zhang SP, Qin N, Flores CM, Isaacsohn I, Varadi M, Mori Y, Jones WK, Schwartz A (2009) Targeted disruption of the voltage-dependent Ca^{2+} channel $\alpha2/\delta$-1 subunit. Am J Physiol Heart Circ Physiol 297:H117–H124. CrossRef Medline

Goldstein ME, House SB, Gainer H (1991) NF-L and peripherin immunoreactivities define distinct classes of rat sensory ganglion cells. J Neurosci Res 30:92–104. CrossRef Medline

Gong HC, Hang J, Kohler W, Li L, Su TZ (2001) Tissue-specific expression and gabapentin-binding properties of calcium channel $\alpha2\delta$ subunit subtypes. J Membr Biol 184:35–43. CrossRef Medline

Gurnett CA, De Waard M, Campbell KP (1996) Dual function of the voltage-dependent Ca^{2+} channel $\alpha_2\delta$ subunit in current stimulation and subunit interaction. Neuron 16:431–440. CrossRef Medline

Hendrich J, Van Minh AT, Heblich F, Nieto-Rostro M, Watschinger K, Striessnig J, Wratten J, Davies A, Dolphin AC (2008) Pharmacological disruption of calcium channel trafficking by the $\alpha2\delta$ ligand gabapentin. Proc Natl Acad Sci U S A 105:3628–3633. CrossRef Medline

Hjerling-Leffler J, Alqatari M, Ernfors P, Koltzenburg M (2007) Emergence of functional sensory subtypes as defined by transient receptor potential channel expression. J Neurosci 27:2435–2443. CrossRef Medline

Hoppa MB, Lana B, Margas W, Dolphin AC, Ryan TA (2012) $\alpha2\delta$ couples calcium channels to neurotransmitter release sites to control release probability. Nature 486:122–125. CrossRef Medline

Ji RR, Strichartz G (2004) Cell signaling and the genesis of neuropathic pain. Sci STKE 2004:reE14. CrossRef Medline

Kato AS, Zhou W, Milstein AD, Knierman MD, Siuda ER, Dotzlaf JE, Yu H, Hale JE, Nisenbaum ES, Nicoll RA, Bredt DS (2007) New transmembrane AMPA receptor regulatory protein isoform, γ-7, differentially regulates AMPA receptors. J Neurosci 27:4969–4977. CrossRef Medline

Khasabov SG, Cain DM, Thong D, Mantyh PW, Simone DA (2001) Enhanced responses of spinal dorsal horn neurons to heat and cold stimuli following mild freeze injury to the skin. J Neurophysiol 86:986–996. Medline

Kim HY, Park CK, Cho IH, Jung SJ, Kim JS, Oh SB (2008) Differential changes in TRPV1 expression after trigeminal sensory nerve injury. J Pain 9:280–288. CrossRef Medline

Klugbauer N, Marais E, Hofmann F (2003) Calcium channel $\alpha2\delta$ subunits: differential expression, function, and drug binding. J Bioenerg Biomembr 35:639–647. CrossRef Medline

Knowlton WM, Palkar R, Lippoldt EK, McCoy DD, Baluch F, Chen J, McKemy DD (2013) A sensory-labeled line for cold: TRPM8-expressing sensory neurons define the cellular basis for cold, cold pain, and cooling-mediated analgesia. J Neurosci 33:2837–2848. CrossRef Medline

Kobayashi K, Fukuoka T, Obata K, Yamanaka H, Dai Y, Tokunaga A, Noguchi K (2005) Distinct expression of TRPM8, TRPA1, and TRPV1 mRNAs in rat primary afferent neurons with aδ/c-fibers and colocalization with trk receptors. J Comp Neurol 493:596–606. CrossRef Medline

Lawson SN (2002) Phenotype and function of somatic primary afferent nociceptive neurones with C-, Aδ- or Aα/β-fibres. Exp Physiol 87:239–244. CrossRef Medline

Li CY, Song YH, Higuera ES, Luo ZD (2004) Spinal dorsal horn calcium channel $\alpha2\delta$-1 subunit upregulation contributes to peripheral nerve injury-induced tactile allodynia. J Neurosci 24:8494–8499. CrossRef Medline

Li CY, Zhang XL, Matthews EA, Li KW, Kurwa A, Boroujerdi A, Gross J, Gold MS, Dickenson AH, Feng G, Luo ZD (2006) Calcium channel $\alpha(2)\delta(1)$ subunit mediates spinal hyperexcitability in pain modulation. Pain 125: 20–34. CrossRef Medline

Li L, Cao XH, Chen SR, Han HD, Lopez-Berestein G, Sood AK, Pan HL (2012) Up-regulation of Cavbeta3 subunit in primary sensory neurons increases voltage-activated Ca^{2+} channel activity and nociceptive input in neuropathic pain. J Biol Chem 287:6002–6013. CrossRef Medline

Marais E, Klugbauer N, Hofmann F (2001) Calcium channel $\alpha(2)\delta$ subunits: structure and gabapentin binding. Mol Pharmacol 59:1243–1248. CrossRef Medline

Minett MS, Nassar MA, Clark AK, Passmore G, Dickenson AH, Wang F, Malcangio M, Wood JN (2012) Distinct Nav1.7-dependent pain sensations require different sets of sensory and sympathetic neurons. Nat Commun 3:791. CrossRef Medline

Moore RA, Straube S, Wiffen PJ, Derry S, McQuay HJ (2009) Pregabalin for acute and chronic pain in adults. Cochrane Database Syst Rev CD007076.

Moore RA, Wiffen PJ, Derry S, McQuay HJ (2011) Gabapentin for chronic neuropathic pain and fibromyalgia in adults. Cochrane Database Syst Rev CD007938.

Newton RA, Bingham S, Case PC, Sanger GJ, Lawson SN (2001) Dorsal root ganglion neurons show increased expression of the calcium channel $\alpha2\delta$-1 subunit following partial sciatic nerve injury. Brain Res Mol Brain Res 95:1–8. CrossRef Medline

Qin N, Olcese R, Stefani E, Birnbaumer L (1998) Modulation of human neuronal α_{1E}-type calcium channel by $\alpha_2\delta$-subunit. Am J Physiol 274: C1324–C1331. Medline

Quick K, Zhao J, Eijkelkamp N, Linley JE, Rugiero F, Cox JJ, Raouf R, Gringhuis M, Sexton JE, Abramowitz J, Taylor R, Forge A, Ashmore J, Kirkwood N, Kros CJ, Richardson GP, Freichel M, Flockerzi V, Birnbaumer L, Wood JN (2012) TRPC3 and TRPC6 are essential for normal mechanotransduction in subsets of sensory neurons and cochlear hair cells. Open Biol 2:120068. CrossRef Medline

R Development Core Team (2012) A language and environment for statistical computing. Vienna: R Foundation for Statistical Computing.

Raghib A, Bertaso F, Davies A, Page KM, Meir A, Bogdanov Y, Dolphin AC (2001) Dominant-negative synthesis suppression of voltage-gated calcium channel $Ca_v2.2$ induced by truncated constructs. J Neurosci 21: 8495–8504. Medline

Ramirez JD, Barnes PR, Mills KR, Bennett DL (2012) Intermediate Charcot-Marie-Tooth disease due to a novel Trp101Stop myelin protein zero mutation associated with debilitating neuropathic pain. Pain 153:1763–1768. CrossRef Medline

Regan LJ, Sah DW, Bean BP (1991) Ca^{2+} channels in rat central and peripheral neurons: high-threshold current resistant to dihydropyridine blockers and omega-conotoxin. Neuron 6:269–280. CrossRef Medline

Rigaud M, Gemes G, Barabas ME, Chernoff DI, Abram SE, Stucky CL, Hogan QH (2008) Species and strain differences in rodent sciatic nerve anatomy: implications for studies of neuropathic pain. Pain 136:188–201. CrossRef Medline

Ruscheweyh R, Forsthuber L, Schoffnegger D, Sandkühler J (2007) Modification of classical neurochemical markers in identified primary afferent neurons with Aβ-, Aδ-, and C-fibers after chronic constriction injury in mice. J Comp Neurol 502:325–336. CrossRef Medline

Saegusa H, Kurihara T, Zong S, Kazuno A, Matsuda Y, Nonaka T, Han W, Toriyama H, Tanabe T (2001) Suppression of inflammatory and neuropathic pain symptoms in mice lacking the N-type Ca^{2+} channel. EMBO J 20:2349–2356. CrossRef Medline

Scroggs RS, Fox AP (1991) Distribution of dihydropyridine and omega-conotoxin-sensitive calcium currents in acutely isolated rat and frog sensory neuron somata: diameter-dependent L channel expression in frog. J Neurosci 11:1334–1346. Medline

Scroggs RS, Fox AP (1992) Calcium current variation between acutely isolated adult rat dorsal root ganglion neurons of different size. J Physiol 445:639–658. Medline

Seltzer Z, Dubner R, Shir Y (1990) A novel behavioral model of neuropathic pain disorders produced in rats by partial sciatic nerve injury. Pain 43:205–218. CrossRef Medline

Sikandar S, Ronga I, Iannetti GD, Dickenson AH (2013) Neural coding of nociceptive stimuli-from rat spinal neurones to human perception. Pain 154:1263–1273. CrossRef Medline

Suzuki R, Rahman W, Rygh LJ, Webber M, Hunt SP, Dickenson AH (2005) Spinal-supraspinal serotonergic circuits regulating neuropathic pain and its treatment with gabapentin. Pain 117:292–303. CrossRef Medline

Taylor CP, Garrido R (2008) Immunostaining of rat brain, spinal cord, sensory neurons and skeletal muscle for calcium channel α2-δ type 1 protein. Neuroscience 155:510–521. CrossRef Medline

Tran-Van-Minh A, Dolphin AC (2010) Gabapentin inhibits the Rab11-dependent recycling of the calcium channel subunit α2δ-2. J Neurosci 130:12856–12867.

Tsujino H, Kondo E, Fukuoka T, Dai Y, Tokunaga A, Miki K, Yonenobu K, Ochi T, Noguchi K (2000) Activating transcription factor 3 (ATF3) induction by axotomy in sensory and motoneurons: a novel neuronal marker of nerve injury. Mol Cell Neurosci 15:170–182. CrossRef Medline

Tuluc P, Kern G, Obermair GJ, Flucher BE (2007) Computer modeling of siRNA knockdown effects indicates an essential role of the Ca^{2+} channel α2δ-1 subunit in cardiac excitation-contraction coupling. Proc Natl Acad Sci U S A 104:11091–11096. CrossRef Medline

Urch CE, Dickenson AH (2003) In vivo single unit extracellular recordings from spinal cord neurones of rats. Brain Res Brain Res Protoc 12:26–34. CrossRef Medline

Wakisaka S, Kajander KC, Bennett GJ (1992) Effects of peripheral nerve injuries and tissue inflammation on the levels of neuropeptide Y-like immunoreactivity in rat primary afferent neurons. Brain Res 598:349–352. CrossRef Medline

Wang H, Sun H, Della PK, Benz RJ, Xu J, Gerhold DL, Holder DJ, Koblan KS (2002) Chronic neuropathic pain is accompanied by global changes in gene expression and shares pathobiology with neurodegenerative diseases. Neuroscience 114:529–546. CrossRef Medline

Watson C, Paxinos G, Kayalioglu G, Heise C (2009) Atlas of the mouse spinal cord. In: The spinal cord, pp 308–379. New York: Academic.

Wyatt CN, Page KM, Berrow NS, Brice NL, Dolphin AC (1998) The effect of overexpression of auxiliary calcium channel subunits on native Ca^{2+} channel currents in undifferentiated NG108–15 cells. J Physiol (Lond) 510:347–360. CrossRef Medline

Zimmermann M (1983) Ethical guidelines for investigations of experimental pain in conscious animals. Pain 16:109–110. CrossRef Medline